

**DEVELOPMENT OF A DIGITAL TWIN FOR THE
CONTROL OF FLOW AND LEVEL SYSTEMS
USING PID AND CASCADE CONTROL
STRATEGIES**

CHANG JIA REN

UNIVERSITI TUNKU ABDUL RAHMAN

**DEVELOPMENT OF A DIGITAL TWIN FOR THE CONTROL OF FLOW
AND LEVEL SYSTEMS USING PID AND CASCADE CONTROL
STRATEGIES**

CHANG JIA REN


**A project report submitted in partial fulfilment of the requirements for the
award of Bachelor of Engineering (Honours) Industrial Engineering**

**Faculty of Engineering and Green Technology
Universiti Tunku Abdul Rahman**

May 2025

DECLARATION

I hereby declare that this project report is based on my original work except for citations and quotations which have been duly acknowledged. I also declare that it has not been previously and concurrently submitted for any other degree or award at UTAR or other institutions.

Signature	:		
Name	:	Chang Jia Ren	
ID No.	:	2101903	
Date	:	25/4/2025	

APPROVAL FOR SUBMISSION

I certify that this project report entitled “**DEVELOPMENT OF A DIGITAL TWIN FOR THE CONTROL OF FLOW AND LEVEL SYSTEMS USING PID AND CASCADE CONTROL STRATEGIES**” was prepared by **CHANG JIA REN** has met the required standard for submission in partial fulfilment of the requirements for the award of Bachelor of Engineering (Honours) Industrial Engineering at Universiti Tunku Abdul Rahman.

Approved by,

Signature

:



Supervisor

:

Dr Leong Sim Siong

Date

:

25/4/2025

The copyright of this report belongs to the author under the terms of the copyright Act 1987 as qualified by Intellectual Property Policy of Universiti Tunku Abdul Rahman. Due acknowledgement shall always be made of the use of any material contained in, or derived from, this report.

© 2025, Chang Jia Ren. All right reserved.

ACKNOWLEDGEMENTS

I would like to convey my profound appreciation to my supervisor, Dr Leong Sim Seong, for his exceptional guidance, assistance, and constructive feedback throughout this entire project. His expertise, insights, and motivation were invaluable to the development and completion of this work.

I would also like to extend my gratitude to my friends, whose support and encouragement provided a source of motivation and perseverance during the various stages of this project. Their understanding, support, and words of reassurance have been a constant source of inspiration, and I am truly grateful for their presence throughout.

Moreover, I am deeply grateful to my family for their unwavering support, patience, and encouragement. Their steadfast belief in my abilities has been a fundamental source of strength throughout this journey.

Finally, I would like to express my deepest appreciation to everyone who has been part of this journey. Your support, encouragement, and belief in me have been irreplaceable, and I am truly grateful for each of you. Whether through direct assistance or moral support, your contributions have made a lasting impact on both my work and my personal growth.

DEVELOPMENT OF A DIGITAL TWIN FOR THE CONTROL OF FLOW AND LEVEL SYSTEMS USING PID AND CASCADE CONTROL STRATEGIES

ABSTRACT

This project presents the development and validation of a digital twin for flow and level control systems, including a cascade control configuration, aiming to enhance educational platforms through sustainable and interactive learning tools. The performance of P, PI, and PID controllers was experimentally evaluated in regulating flow rate, highlighting the trade-offs between steady-state error, overshoot, and system stability. A mathematical model of the physical process was derived using first principles, linearized, and transformed into transfer functions for simulation in MATLAB Simulink. Some parameters were estimated and assumed through comparison with experimental data, achieving close alignment and confirming the model's accuracy for flow control system. Simulations of the flow, level, and cascade control systems revealed that higher proportional gains improved response time but introduced oscillations, while integral and derivative actions contributed to error elimination and improved damping, respectively. The cascade control system demonstrated enhanced stability and responsiveness by addressing disturbances at the inner-loop level. Despite some discrepancies during initial transients, likely due to simplified assumptions and unmodeled disturbances, the digital twin effectively replicates real system behavior and serves as a valuable educational resource for control system learning and analysis.

Keywords: Digital Twin, PID Controller, MATLAB Simulink, Virtual Laboratory, Engineering Education

Subject area: Flow and Level Control Systems

TABLE OF CONTENTS

DECLARATION	iii
APPROVAL FOR SUBMISSION	iv
ACKNOWLEDGEMENTS	vi
ABSTRACT	vii
TABLE OF CONTENTS	viii
LIST OF TABLES	xi
LIST OF FIGURES	xii
LIST OF SYMBOLS / ABBREVIATIONS	xvi

CHAPTER

1	INTRODUCTION	1
1.1	Project Background	1
1.1.1	Process Control	1
1.1.2	Digital Twin	2
1.1.3	MATLAB Simulink	3
1.1.4	Application of Digital Twin in Process Control System	5
1.1.5	Comparison Between Offline and Online Laboratory	5
1.2	Problem Statement	6
1.3	Aim and Objectives	8
1.4	Scope and Limitations	8
2	LITERATURE REVIEW	10
2.1	Introduction	10

2.2	Introduction to Process Control	10
2.3	Proportional, Integral and Derivative (PID) Controller	11
2.4	Control Strategies	13
2.4.1	Feedback Control	13
2.4.2	Feedforward Control	15
2.4.3	Cascade Control	16
2.4.4	On/off Control	18
2.4.5	Model Predictive Control (MPC)	19
2.4.6	Other Control Strategies	21
2.5	Process Modelling: An example of a stirred-tank blending system	22
2.6	Digital Twin	26
3	METHODOLOGY	32
3.1	Introduction	32
3.2	Project Flow	33
3.3	Process Description	34
3.4	Experimental Methods	36
3.5	Modelling and Simulation	37
4	RESULTS AND DISCUSSION	38
4.1	Flow Control Experiment	38
4.1.1	Proportional Controller	38
4.1.2	Integrative Controller	40
4.1.3	Derivative Controller	41
4.2	Process Modelling	43
4.2.1	Modelling of Process and Instruments	43
4.2.1.3	Transmitter	48
4.2.1.4	PID Controller	48
4.2.2	Control Loop	50
4.2.2.1	Flow Control Loop	51
4.2.2.2	Level Control Loop	53
4.2.2.3	Flow/Level Cascade Control Loop	56
4.3	Value Assignment	58

4.3.1	Level Tank	58
4.3.2	I/P Transducer and Control Valve	60
4.3.3	Transmitter	68
4.4	Simulation Results	68
4.4.1	Flow Control	69
4.4.2	Level Control	74
4.4.3	Flow/Level Cascade Control	79
5	CONCLUSION AND RECOMMENDATION	85
5.1	Conclusion	85
5.2	Recommendation	87
	REFERENCES	88

LIST OF TABLES

TABLE	TITLE	PAGE
2.1	Summary of different modelling softwares	29
3.1	Instruments functions	35

LIST OF FIGURES

FIGURE	TITLE	PAGE
2.1	Parallel form of PID controller	12
2.2	Series form of PID controller	12
2.3	Simplified block diagram for feedback control	14
2.4	Simplified block diagram for feedforward control	15
2.5	Simplified block diagram for cascade control	17
2.6	Stirred tank blending system	23
2.7	Block diagram for process dynamics	24
2.8	Feedback control block diagram of stirred tank blending system	25
2.9	Schematic diagram of stirred tank blending system	26
3.1	Project flow chart	33
3.2	Schematic diagram of SOLTEQ® flow/level cascade control trainer (model: SE 465)	34
4.1	Response of flow rate (controlled variable) toward set point change (from 10 LPM to 15 LPM) regulated by proportional controller with different PB values	39
4.2	Response of flow rate (controlled variable) toward set point change (from 10 LPM to 15 LPM) regulated by proportional and integral controller with different I values and constant PB = 150%	40
4.3	Response of flow rate (controlled variable) toward set point change (from 10 LPM to 15 LPM) regulated by proportional, integral, and derivative controller with different D values, constant PB = 150% and $I = 20 \text{ s}^{-1}$	42

4.4	Flow control feedback loop in MATLAB Simulink	51
4.5	Level control feedback loop in MATLAB Simulink	53
4.6	Flow/level cascade control feedback loop in MATLAB Simulink	56
4.7	Simplified flow/level cascade control feedback loop in MATLAB Simulink	57
4.8	Block diagram with transfer function of I/P transducer and control valve	60
4.9	Response of simulated and experimental flow rate (controlled variable) toward the set point change (from 10 LPM to 15 LPM) at $K_{IP}K_v = 0.5 \frac{LPM}{mA}$ and $\tau_v = 2.3$ regulated by proportional controller	61
4.10	Response of simulated and experimental flow rate (controlled variable) toward the set point change (from 10 LPM to 15 LPM) at $K_{IP}K_v = 1 \frac{LPM}{mA}$ and $\tau_v = 2.3$ regulated by proportional controller	62
4.11	Response of simulated and experimental flow rate (controlled variable) toward the set point change (from 10 LPM to 15 LPM) at $K_{IP}K_v = 0.5 \frac{LPM}{mA}$ and $\tau_v = 2.3$ regulated by proportional and integral controller	63
4.12	Response of simulated and experimental flow rate (controlled variable) toward the set point change (from 10 LPM to 15 LPM) at $K_{IP}K_v = 1 \frac{LPM}{mA}$ and $\tau_v = 2.3$ regulated by proportional and integral controller	63
4.13	Response of simulated and experimental flow rate (controlled variable) toward the set point change (from 10 LPM to 15 LPM) at $K_{IP}K_v = 1 \frac{LPM}{mA}$ and $\tau_v = 0.2$ regulated by proportional controller	64
4.14	Response of simulated and experimental flow rate (controlled variable) toward the set point change (from 10 LPM to 15 LPM) at $K_{IP}K_v = 1 \frac{LPM}{mA}$ and $\tau_v = 1.5$ regulated by proportional controller	65
4.15	Response of simulated and experimental flow rate (controlled variable) toward the set point change (from 10 LPM to 15 LPM) at $K_{IP}K_v = 1 \frac{LPM}{mA}$ and $\tau_v = 2.3$ regulated by proportional controller	65

4.16	Response of simulated and experimental flow rate (controlled variable) toward the set point change (from 10 LPM to 15 LPM) at $K_{IP}K_v = 1 \frac{\text{LPM}}{\text{mA}}$ and $\tau_v = 0.2$ regulated by proportional and integral controller	66
4.17	Response of simulated and experimental flow rate (controlled variable) toward the set point change (from 10 LPM to 15 LPM) at $K_{IP}K_v = 1 \frac{\text{LPM}}{\text{mA}}$ and $\tau_v = 1.5$ regulated by proportional and integral controller	67
4.18	Response of simulated and experimental flow rate (controlled variable) toward the set point change (from 10 LPM to 15 LPM) at $K_{IP}K_v = 1 \frac{\text{LPM}}{\text{mA}}$ and $\tau_v = 2.3$ regulated by proportional and integral controller	67
4.19	Response of simulated (controlled variable) toward the set point change (from 10 LPM to 15 LPM) regulated by proportional controller with different P values	69
4.20	Comparison of simulated and experimental flow rate (controlled variable) toward the set point change (from 10 LPM to 15 LPM) regulated by proportional controller with different P values	70
4.21	Response of simulated flow rate (controlled variable) toward the set point change (from 10 LPM to 15 LPM) regulated by proportional and integral controller with different I values and constant P = 0.67	71
4.22	Detailed view of early-stage system response in Figure 4.21	71
4.23	Comparison of simulated and experimental flow rate (controlled variable) toward the set point change (from 10 LPM to 15 LPM) regulated by proportional and integral controller with different I values and constant P = 0.67	72
4.26	Response of simulated flow rate (controlled variable) toward the set point change (from 10 LPM to 15 LPM) regulated by proportional, integral and derivative controller with different D values and constant P = 0.67, I = 20 s ⁻¹ , and N = 3	73
4.25	Detailed view of early-stage system response in Figure 4.24	73
4.26	Comparison of simulated and experimental flow rate (controlled variable) toward the set point change (from 10 LPM to 15 LPM) regulated by proportional, integral and derivative controller with different D values and constant P = 0.67, I = 20 s ⁻¹ , and N = 3	74

4.27	Response of simulated liquid level (controlled variable) toward the set point change (from 10 LPM to 15 LPM) regulated by proportional controller at different P values	75
4.28	Response of simulated liquid level (controlled variable) toward the set point change (from 10 LPM to 15 LPM) regulated by proportional and integral controller with different I values and constant $P = 1$	76
4.29	Detailed view of early-stage system response in Figure 4.28	77
4.30	Response of simulated liquid level (controlled variable) toward the set point change (from 10 LPM to 15 LPM) regulated by proportional, integral, and derivative controller with different D values and constant $P = 1$, $I = 0.2 \text{ s}^{-1}$ and $N = 3$	78
4.31	Detailed view of early-stage system response in Figure 4.30	78
4.32	Response of simulated liquid level (controlled variable) toward the set point change (from 10 LPM to 15 LPM) regulated by proportional controller with different P_I values	80
4.33	Response of simulated liquid level (controlled variable) toward the set point change (from 10 LPM to 15 LPM) regulated by proportional and integral controller with different I_I values and constant $P_I = 1$	81
4.34	Detailed view of early-stage system response in Figure 4.33	82
4.35	Response of simulated liquid level (controlled variable) toward the set point change (from 10 LPM to 15 LPM) regulated by proportional, integral, and derivative controller with different D values and constant $P_I = 1$ and $I_I = 0.2 \text{ s}^{-1}$	83
4.36	Detailed view of early-stage system response in Figure 4.35	83

LIST OF SYMBOLS / ABBREVIATIONS

Y_{sp}	set point
D	disturbance
Y	controlled variable in feedback control system
Y_{sp1}	set point of primary loop in cascade control system
Y_{sp2}	set point of secondary loop in cascade control system
D_1	disturbance of primary loop
D_2	disturbance of secondary loop
Y_1	output of secondary loop
Y_2	output of secondary loop
x_1	mass fraction of chemical A in stream 1 of stirred-tank blending system
x_2	mass fraction of chemical A in stream 2 of stirred-tank blending system
w_1	mass flow rate of chemical A in stream 1 of stirred-tank blending system
w_2	mass flow rate of stream 2 in stirred-tank blending system
x	mass fraction of chemical A in output of stirred-tank blending system
w	mass flow rate of output of stirred-tank blending system
x_{sp}	set point of stirred-tank blending system
K_m	transmitter gain
G_c	feedback controller transfer function
G_{IP}	current-to-pressure transducer transfer function
G_v	control valve transfer function
G_p	process tank transfer function
G_m	analyzer and transmitter (sensor)

A	area of level tank, m^2
h	height of liquid in the level tank, m
\bar{h}	steady state height of liquid in level tank, m
q_i	input stream, LPM
\bar{q}_i	steady state input flow rate, LPM
q	output stream, LPM
C_v	valve coefficient
N	conversion unit $\frac{gpm}{psi^{\frac{1}{2}}}$
$f(l)$	valve opening, %
Δp_v	pressure drop across valve
g_s	specific gravity of water
K_p	level tank process gain
K_{IP}	current-to-pressure transducer gain
K_v	control valve gain
K_m	flow transmitter gain
K_l	level transmitter gain
K_c	controller gain
τ_p	level tank time constant, s
τ_v	control valve time constant, s
τ_I	integral controller time constant, s
τ_D	derivative controller time constant, s
N	derivative filter
α	a constant between 0.05 and 0.1
G_{c1}	primary controller
G_{c2}	secondary controller
P_1	primary proportional gain
I_1	primary integral gain, s^{-1}
D_1	primary derivative gain, s
P_2	secondary proportional gain
I_2	secondary integral gain, s^{-1}
D_2	secondary derivative gain, s
F_{sp}	step change input of flow (secondary) control loop, LPM

X_{sp}	set point of flow (secondary) control loop, LPM
E	error input of PID controller in flow (secondary) control loop, mA
P	output of PID controller in flow (secondary) control loop, mA
F	output flow rate response in flow (secondary) control loop, LPM
F_m	output of flow transmitter in flow (secondary) control loop, mA
X	bias in flow (secondary) control loop, LPM
U	actual output flow rate in flow (secondary) control loop, LPM
H_{sp}	step change input of level (primary) control loop, mm
Y_{sp}	set point of level (primary) control loop, LPM
T	error input of PID controller in level (primary) control loop, mA
S	output of PID controller in level (primary) control loop, mA
W	output of control valve in level (primary) control loop, LPM
H	output of level tank in level (primary) control loop, mm
H_l	output of level transmitter in level (primary) control loop, mA
Y	bias in level (primary) control loop, mA
L	actual output water level in level (primary) control loop, mm
AI	Artificial Intelligence
IoT	Internet-of-Things
PB	proportional band, %
P	proportional gain
I	integral gain, s^{-1}
D	derivative gain or derivative time, s
MPC	model predictive controller
HVAC	heating, ventilation and air conditioning system
BMS	building management system
MIMO	multiple-input, multiple-output
OPC UA	open platform communications unified architecture
RUL	remaining useful life
MIL	model-in-the-loop
ODE	ordinary differential equation

CHAPTER 1

INTRODUCTION

1.1 Project Background

Section 1.1 explains the background of the project, which includes process control, digital twin, MATLAB Simulink, application of digital twin in process control and comparison between offline and online laboratory. Section 1.2 and 1.3 explains the problem statement and objectives of this study. Section 1.4 covers the scope and limitations of this project

1.1.1 Process Control

Process control aims to enhance process safety, satisfy environmental constraints and reduce pollution, meet product quality specifications, minimize operating costs, and maintain a process's intended operating parameters (Seborg et al., 2016). Process control systems gather, store, and analyze real-time data from controllers and other connected automation systems. This historized data are beneficial in displaying trends in a process over time or in identifying the root cause of process disturbances (Harbud, 2022). Process variables involved in a control system are controlled variables, manipulated variables and disturbance variables. Some examples of process variables include composition, temperature, pressure and flow rates. Process control works based on the principle of continuously monitoring process variables and making

adjustments to maintain desired operating conditions. Control systems use sensors to measure process variables, compare them to setpoints, and apply corrective actions through controllers to minimize deviations and ensure stable operation. Some of the simplest process control strategies are feedback control strategy, feedforward control strategy, the combination of feedback and feedforward control strategy, and cascade control strategy (Seborg et al., 2016).

1.1.2 Digital Twin

A generalized definition for a digital twin is a virtual representation of a physical system that is updated through the exchange of information between physical and virtual systems. There are three characteristics a digital twin consists of: (i) a physical reality, (ii) a virtual representation, and (iii) interconnections that enables two-way communication between the physical reality and the virtual representation. The physical reality is a general way to represent the system that is to be modeled. This includes the physical system, physical environment, and physical processes. The physical system is made up of a group of interacting and interrelated entities that form a unified whole. The physical environment is what surrounds the physical system and influences the physical system through external factors such as room temperature, air flow, vibration or others. Physical processes are how the physical system reacts to the changes in the environment which subsequently leads to changes in state over time. The virtual representation is a data model that mirrors an idealized form of the physical reality in a virtual space. Likewise, there are also the virtual system, virtual environment and virtual processes in the virtual representation. The last characteristic of a digital twin is the exchange of information between the physical reality and the virtual representation. The physical-to-virtual connection involved data collection in the physical reality, interpretation of the collected data, and update the states in the virtual representation. On the other hand, virtual-to-physical connection closes the loop in the digital twin by transferring information from the virtual representation to the physical reality. This allows decisions generated in the virtual representation to be implemented in the physical reality (VanDerHorn and Mahadevan, 2021).

Digital twin technology can be used in different sectors such as healthcare, maritime and shipping, manufacturing, city management and aerospace (Semeraro, 2021). Through simulation of scenarios, it determines better therapy options; improve structural and functional components of a ship, prediction of equipment failures, improve urban environment and quality of life, enhance safety and security, carry out predictive maintenance and reduce cost. There are still some drawbacks of virtual models even though digital twins have very big influences. According to Pires et al. (2019), the lack of methodologies and techniques for validation against real processes causes it to be time consuming and difficult. The second challenge is the difficulty in unification and exchange of information within a company. Lack of knowledge and skills about digital engineering and organization of the company structure lead to difficulties in accessing information from different structures. The third challenge is to establish real-time connection and synchronization between the virtual and physical model. This is namely due to the variability, uncertainties and fuzziness of the physical environment. This induces doubt towards these systems to perform autonomous decisions.

1.1.3 MATLAB Simulink

Researchers usually prefer to develop their models in a real-time environment and MATLAB Simulink provides a graphical programming environment for modeling, simulating, and analyzing dynamic systems. It allows users to create block diagrams to represent systems, enabling simulation of their behavior over time, and supports model-based design for control systems and signal processing. MATLAB Simulink provides a user-friendly graphical interface for building complex models using block diagrams, making it easier to visualize system dynamics. Besides, it allows for real-time simulation and testing of models, enabling engineers to identify issues early in the design process and optimize performance. It also seamlessly integrates with MATLAB for advanced data analysis and algorithm development, and supports various toolboxes for specialized applications, enhancing its versatility in engineering projects. MATLAB Simulink is commonly used in engineering fields such as control

systems, signal processing, communications, and robotics for design, testing, and validation of algorithms and systems (Mikkili et al., 2015).

Simulation tools are very important as the demand in the automotive electronics, disk drive electronics and robotics industry are increasing for Industry 4.0. Kiyakli and Solmaz (2019) created and simulated a dynamic model of an electric vehicle using MATLAB Simulink to test its reliability. They successfully conducted this study and concluded that the energy consumption, vehicle speed and cycle speed are correct for both NEDC and WLTP cycles. Besides, Shukla et al. (2015) developed a program in MATLAB Simulink for a 36W photovoltaic module. This software allows simulation of the PV module for prediction and validation of its' behaviour under varying temperature and solar radiation. The research was a success as the accurateness of the simulated results were validated with the manufacturers results.

Simulation tools are incorporated in the development of digital twins. Bilansky et al. (2023) describe how a digital twin of a Li-ion battery cell was developed using MATLAB Simulink based on measured data. The designed digital twin was then tested and compared against a generic MATLAB Simulink model, which represents an empirical battery cell model, to assess accuracy. The comparison involved the dynamics of the real battery cell, the developed digital twin in MATLAB Simulink, and the generic model. The results showed that the digital twin was more accurate under steady-state conditions, but less accurate during dynamic current changes. It was recommended that accuracy could be improved by collecting more dynamic test data, such as through the implementation of Hybrid Pulse Power Characterization (HPPC) and micro-cycling. This would enhance the dataset and lead to more realistic parameter estimation.

1.1.4 Application of Digital Twin in Process Control System

Digital twins are widely used to optimize control in process systems integrating virtual modelling, monitoring, diagnosis, and control. He et al. (2019) emphasizes the control of digital twins in monitoring, diagnosing, and optimizing control in industrial automation. It highlights how digital twins can simulate physical systems, manage process faults, and enhance operational safety and efficiency. The three types of failures addressed include sensor faults, actuator failures, and process disturbances, while optimized control configurations and adaptive algorithms for real-time and offline optimization were proposed. The findings indicate that the digital twin system enhances safety, reduces operational fluctuations, and improves fault tolerance in industrial process control systems.

1.1.5 Comparison Between Offline and Online Laboratory

Traditional education for laboratory sessions is no longer as effective as it once was. Technology has been advancing at a rapid pace, and traditional laboratories are struggling to keep up with modern industry requirements. Although physical laboratories allow face-to-face sessions, they come with numerous limitations. Not only do they have restricted resources, but they also suffer from limited accessibility. There is often an insufficient number of equipment, leaving some students merely observing rather than actively participating. Furthermore, students are constrained by the laboratory hours, limiting opportunities to conduct experiments. Additionally, there may not be enough qualified faculty members to supervise all experiments (Kathane et al., 2013). The high costs of maintaining outdated equipment and the safety concerns associated with physical experiments are undeniable. The limited availability of equipment makes it difficult to accommodate large groups of students, leading to scalability challenges (Faulconer and Gruss, 2018).

In contrast, online laboratory sessions provide 24/7 availability and accessibility. They can be extensively utilised for virtual teaching, e-learning, and other computer-

based education. They allow students to repeat experiments as many times as they wish without any safety risks. Additionally, online laboratories are cost-effective and highly scalable. Moreover, they promote inclusivity by offering equal opportunities to all students, regardless of time and location. The integration of modern technology in online laboratories enhances growth potential, enabling remote operations and collaboration. In some cases, students can even monitor their experimental progress in real-time from a remote location (Faulconer and Gruss, 2018).

1.2 Problem Statement

Today's rapidly digitalizing world makes it crucial to discover and adopt sustainable methods to improve education experience specifically. The integration of technology into education frameworks is no longer a trend but a necessity to be on par with the evolving demands of the digital era. Although education continues to evolve, it has not kept pace with digitalization. It is still not advancing fast enough to be in conjunction with the digitalizing world. Pires et al. (2019) suggested that Industry 4.0 have triggered concepts such as the digital twin, Artificial Intelligence (AI) and Internet-of-Things (IoT). The concept of digital twin is widely applied especially in the manufacturing sector. Consequently, the development of digital twins that can conduct simulations of real time experiments are essential in education. Nowadays, most institutes in the education sector still cling onto their old ways and are not implementing technologies that have been integrated into modern industries, leading to inefficiencies and students not grasping and utilizing the technology until they work in the relevant industries. These digital models that are replicas of real models can provide a dynamic and interactive platform for students to engage with complex systems and foster a deeper understanding with hands-on experience without constraints and risks associated with physical equipment. Furthermore, educational institutions can effectively utilize resources by implementing digital twins that can be reused indefinitely with minimal maintenance, and most importantly allowing multiple students to participate simultaneously. This approach significantly reduces the need for physical materials, equipment, and energy consumption traditionally required for

hands-on learning. By minimizing waste and optimizing resource usage, digital twins contribute to a more sustainable and environmentally conscious education system. Developing virtual real-time models also sparks innovative and creative ideas within the students, allowing them to explore and refine their solutions iteratively. Hence, investing time, talents and capital into digital twins present educational institutions with more flexible, scalable and immersive learning experiences, ultimately prepare students for technological challenges of the future.

In conjunction with this situation, this project aims to develop a comprehensive digital twin of the existing physical education equipment of flow and level control system that can enable students to conduct the experiments in a virtual mode while obtaining feedback or result that imitate the real time experiment. Experiments are first conducted by using the existing educational equipment (flow and level control system) to collect real time experimental data. Then, the mathematical model of the control system is formulated by using the first principle, which is then transformed to the transfer functions in a block diagram in MATLAB Simulink. The model is then simulated to collect the response resulted from the model calculation. The response is analyzed and the model is validated by comparing the response with the real time experimental data. With the validated digital twin model, the parameters/settings of the control system can be adjusted to observe the responses of the system under different circumstances without the need to conduct the experiment by using the real time equipment. The digital twin model will be more cost-effective and accessible to everyone, accommodating various educational settings whether online or physical classes. This way, students can engage in learning together instead of taking turns waiting for the equipment. Therefore, this project will be beneficial to the education sector as it is more flexible and provides a more interactive experience to students.

1.3 Aim and Objectives

This final year project aims to digitalize PID and cascade control education for the flow and level control systems through the development of a digital twin utilizing MATLAB Simulink. The four objectives are as follows:

- i) To evaluate the performance of P, PI, and PID controllers in regulating flow rate under various controller settings through experimental analysis.
- ii) To develop mathematical models for the flow control system, level control system, and cascade control system.
- iii) To simulate the developed control system models using Simulink software.
- iv) To assess the performance of the control systems in controlling the liquid level in the tank under different controller settings by simulation.

1.4 Scope and Limitations

The scope of this project revolves around designing a MATLAB-based digital twin for flow and level control systems using PID and cascade control strategies. It focuses on creating a comprehensive, accurate and engaging model that improves learning experience solely for students. The digital twin for flow and level control systems will include components such as tanks, sensors, controllers, and a source.

The control system utilized is PID controller with feedback and cascade control strategies. The feedback control strategy gives corrective action after the system is being disturbed and cascade control strategies can quickly correct any disturbances in the inner control loop are incorporated in this project. Other strategies such as fuzzy logic controllers that can handle disturbances better than PID controllers are not considered nor used in this project.

The digital twin is only built for the control of flow and level systems. Temperature and pressure are not considered in the system. Besides, this project only

uses MATLAB Simulink for the development and simulation of the virtual model. Any other real-time simulation software is not tested in this project.

Responses that will be collected in this project include the response of water flow rate towards change in the set point of the water pump. The responses using feedback and cascade control strategies may consist of rise time, overshoot, oscillation around the set point, damping, and the time taken to achieve a steady-state flow rate.

The experiments conducted will focus solely on flow control. Level control and flow/level cascade control experiments will not be performed. Disturbances affecting flow control will not be considered during the process modelling, and certain instrument gains will be assumed due to the lack of available data.

The success of this project is determined through the accuracy and stability of the simulated data compared to the real data, and the proficiency of it as an educational tool. All constraints and limitations have been evaluated based on the problem statement, aim and objectives.

CHAPTER 2

LITERATURE REVIEW

2.1 Introduction

This chapter discusses process control in depth, encompassing the different control strategies and the PID controller. Furthermore, Section 2.5 depicts an example of process modelling and Section 2.6 discusses the relationship between digital twins and real-time simulation.

2.2 Introduction to Process Control

The goal of process control is to ensure safe and cost-effective operation while adhering to environmental and product quality standards. In complex processing systems like oil refineries and ethylene plants, thousands of process variables such as compositions, temperatures, and pressures are monitored and regulated. Fortunately, many of these variables can be adjusted to meet these objectives. The three main categories of processes are continuous, batch, and semibatch. Continuous processes include tubular heat exchanger, where the exit temperature of a process fluid is regulated by adjusting the cooling water flow rate, while disturbances like variations in inlet temperatures and flow rates impact performance. In a continuous stirred-tank reactor, where exothermic reactions occur, reactor temperature is controlled by manipulating coolant flow, with feed conditions potentially acting as either control or

disturbance variables. Similarly, in a thermal cracking furnace, the furnace temperature and excess air levels are managed by adjusting fuel flow and fuel/air ratio, with crude oil composition and fuel quality as common disturbances. In a kidney dialysis unit, blood flow is maintained by a pump, and ambient conditions are controlled by adjusting flow rates to ensure the removal of waste products to acceptable levels (Seborg et al., 2016).

The three types of variables that have to be identified in a process control problem are controlled variables, manipulated variables and disturbance variables. The controlled variable is a desired value that the system aims to maintain usually known as the set point. The manipulated variable is a parameter that can be adjusted to influence the controlled variable and maintain it at or near to the desired set point. Normally, manipulated variables are factors such as flow rates, valve positions, or power inputs that can be directly changed by finite control elements within the system. Disturbance variables are parameters that can influence controlled variables but cannot be directly changed. Disturbance variables typically arise from changes in the external environment or fluctuations within the process itself, such as variations in raw material quality, ambient temperature, or feed conditions. These disturbances can cause the controlled variable to deviate from its desired set point (Seborg et al., 2016).

2.3 Proportional, Integral and Derivative (PID) Controller

PID control employs three modes—proportional, integral, and derivative—each contributing uniquely to the control output. The proportional term (P) adjusts the output based on the current error, which is the difference between the setpoint and the process variable. The integral term (I) accumulates past errors over time to reduce any offset, ensuring the process variable reaches the desired setpoint. The derivative term (D) responds to the rate of change in the process variable, allowing for adjustments when there are sudden variations. These three control actions are tuned to achieve optimal performance, making PID controllers widely popular in various industries, such as motion control, process control, and manufacturing, due to their simplicity,

effectiveness, and favorable cost-benefit ratio. PID controllers are also applied to modern technologies like self-driving cars, UAVs, and autonomous robots. They account for 90-95% of control loops in most applications (Borase et al., 2021)

The two common structures for PID controllers are the parallel type, where P, I, and D actions occur in separate terms, and the series type, where changes in gain affect all three actions interactively. In practical applications, finding a perfect model is challenging, so manipulation and trial-and-error methods remain valuable. For example, if a control loop is overly aggressive and causes excessive oscillation, reducing the gain can help. This adjustment slows the response but adds robustness to the loop, making it more stable (Borase et al., 2021). Figure 2.3.1 and Figure 2.3.2 shows the block diagram of the parallel form and series form of PID control.

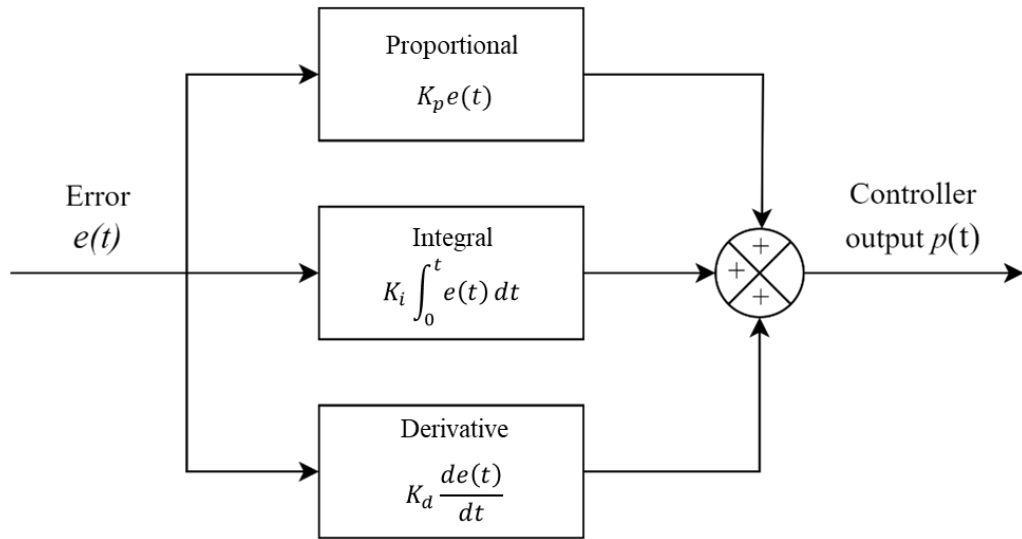


Figure 2.1: Parallel form of PID controller

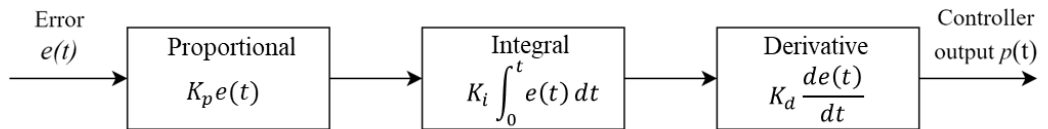


Figure 2.2: Series form of PID controller

Padula et al. (2017) conducted the optimization of PID control for regulating the depth of hypnosis in anesthesia by using propofol administration and the bispectral

index. The study also explored the optimal PI controller tuning using the same methodology as PID controller. Optimal tuning parameters were determined for both controllers. However, it was evident that PID controller outperforms the PI controller and model predictive controller (MPC). PID controller was able to achieve faster induction time and maintain a similar maximum overshoot compared to MPC. The performance of the PI controller that lacks the derivative action is inferior to MPC. These findings suggest that any advanced control strategy for regulating anesthesia should be benchmarked against optimally tuned PID controllers, as they deliver faster induction time with acceptable overshoot and satisfactory disturbance rejection.

2.4 Control Strategies

This section explains different control strategies including feedback control, feedforward control, cascade control, on/off control, model predictive control, and other control strategies.

2.4.1 Feedback Control

Feedback control system plays a major role by comparing measurements to target values and making necessary adjustments to the controlled variables. It involves measuring the controlled variable and using that measurement to adjust the manipulated variable. The disturbance variable is not measured. Feedback control ensures that corrective actions are taken to keep the controlled variable close to its set point. Negative feedback is preferred as the controller will correct deviations, while positive feedback means that the controller amplifies errors and causes the controlled variable to deviate more. The main advantages of feedback control include its ability to handle disturbances from any source and reduce sensitivity to unmeasured disturbances. However, a key limitation is that corrective action only occurs after a

disturbance has already caused the controlled variable to deviate from the set point (Seborg et al., 2016).

Figure 2.3 below shows a simplified block diagram of a feedback control system, where the controlled variable, Y , is measured and compared with the setpoint, Y_{sp} , to make corrective adjustments. The disturbance, D , is not measured, and corrective action is taken regardless of the source of the disturbance.

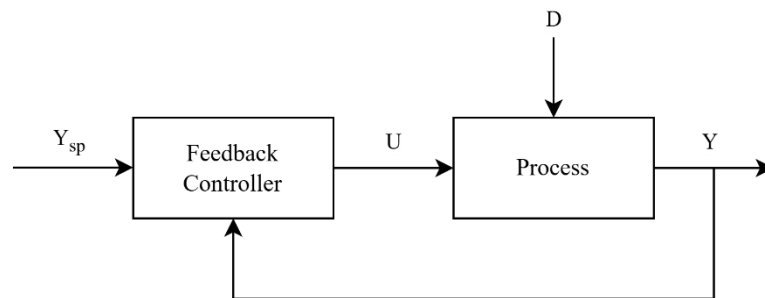


Figure 2.3: Simplified block diagram for feedback control

Yang et al. (2019) summarized the key components surrounding force feedback and control during robot-assisted needle insertion. This included reviewing state-of-the-art force modelling, measurement methods, factors influencing interaction forces, parameter identification, and force control algorithms. The study aimed to enhance the precision and effectiveness of needle insertion procedures in minimally invasive surgeries by improving the force control mechanisms. Feedback control is crucial in this study for reducing tissue deformation and needle deflection during insertion. It provides the surgeon with better control over surgical instruments by integrating force feedback systems that respond to the interaction between the needle and tissue. The study explores various control algorithms and strategies that enable real-time adjustments based on the forces detected during the insertion process. Feedback control in needle insertion enhanced precision by allowing real-time adjustments, improving trajectory and depth accuracy. It reduces tissue deformation and compensates for needle deflection, ensuring the needle stays on the intended path through monitoring and controlling. Surgeons also benefit from force feedback thus gaining better control and making informed decisions during the procedure. Advanced feedback systems can autonomously adapt to unforeseen circumstances, improving safety and effectiveness.

2.4.2 Feedforward Control

Feedforward control is characterized by measuring the disturbance variable instead of the controlled variable. This approach offers a significant advantage, that is the corrective action can be taken preemptively, which is before the controlled variable deviates from its set point. Ideally, this corrective action would completely counteract the effects of the disturbance, ensuring that the controlled variable remains unaffected. Although perfect cancellation of disturbances is generally not achievable, feedforward control can still greatly mitigate the impact of measured disturbances. However, there are a few drawbacks to this method. First, it requires that the disturbance variable be accurately measured or estimated. Second, it does not provide corrective action for disturbances that are not measured. Third, the implementation of feedforward control necessitates an accurate process model, which can add complexity. For example, in a blending system, a feedforward control strategy may not account for unmeasured disturbances in certain inputs, such as the mass flow rate of input stream 1, which consists of a mixture of two chemicals, A and B. While it is theoretically possible to manage this by measuring the mass fraction of chemical A and the mass flow rate of input stream 1 and then adjusting the mass flow rate of input stream 2 accordingly, it is often impractical in industrial applications to measure every potential disturbance variable due to economic constraints (Seborg et al., 2016).

Figure 2.4 shows a simplified block diagram of a feedforward control system, where the disturbance D is measured and used, along with the setpoint Y_{sp} , to make corrective adjustments. The controlled variable, Y , is not measured, and corrective action is taken in advance, before the disturbance causes any deviation from the setpoint.

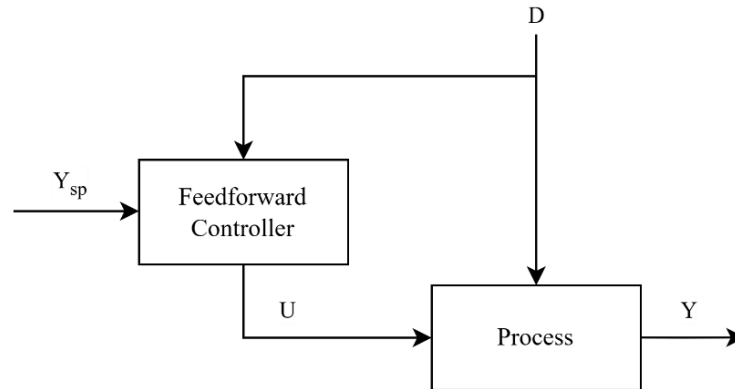


Figure 2.4: Simplified block diagram for feedforward control

Wu et al. (2021) developed an iterative learning method for accurate dynamic feedforward control of industrial hybrid robots by combining a standard dynamic model with iterative learning control (ILC) to optimize feedforward parameters. The study aimed to reduce motion errors and improve tracking performance by addressing uncertainties in the robot's dynamic characteristics. Feedforward control in this study is used to compensate for external dynamic disturbances affecting the robot's performance. The disturbances include external forces acting on the robot that can affect its motion and accuracy, variations in the environment or system that are difficult to predict or model accurately, elastic deformation in the robot's structure under load that can impact its performance and transmission system clearance which are mechanical gaps in the robot's joints and connections that can introduce errors in motion control. Experiments on a 5-DOF hybrid robot showed a reduction in average position errors from 0.18 mm to 0.06 mm with a 66% improvement.

2.4.3 Cascade Control

Another method that can improve how the system responds to disturbances is known as cascade control which involves using a secondary measured variable and a secondary feedback controller. This secondary variable is placed to detect disturbances earlier than the main controlled variable, even if the disturbances themselves aren't directly measured. This approach is widely used in process industries and is

particularly effective when disturbances are related to the manipulated variable or when the final control element doesn't behave in a straightforward manner. The cascade control loop has two main characteristics: the primary controller's output serves as the set point for the secondary controller, and the two feedback loops are arranged with the secondary loop nested within the primary loop. This means there are two controlled variables and two sensors, all managing one manipulated variable. In contrast, a conventional control structure only has one controlled variable, one sensor, and one manipulated variable. The primary advantage of the cascade control strategy is that it positions a second measured variable near a major disturbance, enabling its feedback loop to respond swiftly and improve the system's overall response (Seborg et al., 2016).

Figure 2.5 shows a simplified block diagram of a cascade control system, which consists of two feedback loops. The secondary loop is nested within the primary loop, and the output of the primary controller, Y_{sp2} , serves as the setpoint for the secondary loop. The secondary loop can detect disturbances, D_2 and apply corrective actions more quickly, thereby reducing the response time of the primary feedback loop. Finally, the output Y_1 is compared with the setpoint of the primary loop, Y_{sp1} , and then used as the input to the secondary loop.

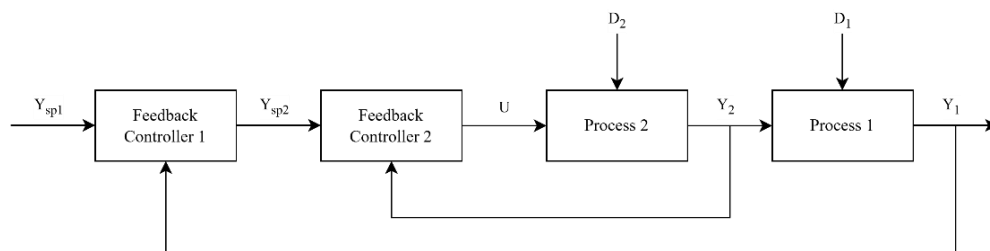


Figure 2.5: Simplified block diagram for cascade control

A study by Ito et al. (2018) aimed to regulate the flow rate from the ladle and maintain the liquid level in the mold sprue cup using a feedback control system that relies on visual measurement at the sprue cup. In the proposed cascade control system, the primary (outer) loop manages the liquid level in the sprue cup, while the secondary (inner) loop controls the flow rate from the pouring ladle. Simulations were conducted to validate the system's performance by comparing it against reference models, both

with and without modelling errors. The simulations revealed that the control outputs for both flow rate and liquid level closely matched the reference models, confirming the effectiveness of the proposed cascade control system. The study's results demonstrated that the proposed system successfully maintained the desired liquid level in the mold sprue cup, even in the presence of modelling errors and disturbances. The system proved to be robust in controlling the ladle's flow rate and minimizing the impact of decreased discharge coefficients.

2.4.4 On/off Control

On-off controllers are the simplest and inexpensive feedback controllers used as thermostats in household heating systems and refrigerators. They are also utilized in non-critical industrial applications, including level control loops and heating systems. On-off controllers are not as extensively utilized as PID controllers in the critical industrial applications due to their limited versatility and effectiveness (Seborg et al., 2016). On-off controllers face several challenges, including the potential for significant overshoot and oscillation around the setpoint due to their binary switching nature, particularly in systems with inherent lag. The presence of hysteresis, where there is a difference between the turn-on and turn-off levels, can cause the controlled variable to fluctuate within a range instead of settling at a precise value. Additionally, on-off controllers offer limited control quality, making them less suitable for applications that require high precision and stability, especially in systems with stringent control demands (Urica et al., 2019). The study by Ardabili et al. (2016) of comparing fuzzy and on/off controllers in a mushroom growing hall also proved that on/off controllers have higher standard deviation, variance, and error compared to fuzzy controllers. Both controllers were used to control temperature, humidity and CO₂ parameters. On/off controllers resulted in bigger fluctuation when controlling the process, higher energy consumption, and a further value from the set point compared to fuzzy control.

Urica et al. (2019) focused their study on the control of stable, 2nd order, continuous systems with overdamped step response. The aim is to enhance the fixed frequency mode of an on-off controller by introducing a hybrid mode that combines the advantages of both comparative and fixed frequency modes. The three control algorithms of the on-off controller used are comparative mode, fixed frequency mode, and hybrid mode. They differ in their approach to managing output. The comparative mode switches the controller output based on the comparison between the desired and actual states, offering faster response times but often resulting in higher overshoots and oscillations. The fixed frequency mode controls the output using a calculated duty cycle and frequency, providing smoother regulation without overshoot, though it has a longer settling time compared to the comparative mode. The hybrid mode combines the advantages of both comparative and fixed frequency modes, delivering enhanced control quality and dynamics while minimizing overshoot, effectively balancing speed and stability better than the other two modes. The results show that the comparative mode offers good speed of control with a settling time of approximately 1.5 seconds but can experience high overshoots, reaching up to 17.5%. The fixed frequency mode provides better quality of regulation with no overshoot, but has a longer settling time, typically between 3.12 to 2.5 times longer than the comparative mode. The hybrid mode achieved the best control quality with optimized settling time and reduced overshoot when the interruption time is set correctly.

2.4.5 Model Predictive Control (MPC)

Model Predictive Control (MPC) is an advanced control strategy that uses a mathematical model to predict future behaviour and optimize control inputs of a system over a specified time horizon. It solves an open-loop optimal control problem at each time step, adjusting control set-points dynamically based on current and predicted conditions to determine the best control inputs. MPC is particularly effective in managing complex systems such as heating, ventilation and air conditioning (HVAC) system where traditional linear control methods may fail. However, MPC relies on accurate data-driven building models where inaccuracies can lead to suboptimal

control performance and energy inefficiencies. Besides, the optimization process can be computationally intensive, requiring significant processing power and time, especially in real-time applications (Joe and Karava, 2019). These challenges were also brought up by Wang et al. (2015) that the effectiveness of MPC heavily relies on the accuracy of the system model and solving the optimization problem at each time step can be computationally intensive, especially for nonlinear systems or large-scale problems, leading to delays in control actions.

Joe and Karava (2019) evaluated the performance of an on-line MPC strategy implemented in an office building with a radiant floor system, focusing on energy use reduction and cost savings under realistic operational conditions. The study involved selecting and setting up three open-plan office spaces on a university campus, with one space equipped with a radiant floor system and the others with conventional air delivery systems. Sensors were installed to collect data on temperature, energy consumption, and HVAC performance during both cooling and heating seasons. This data was used to create data-driven building models that accurately represented the thermal dynamics of the spaces. MPC strategy was then implemented within the Building Management System (BMS) to optimize heating and cooling in real-time. The study found that the radiant floor system with MPC achieved significant energy and cost savings, with reductions of approximately 34% in cooling costs compared to simulated feedback control and 16% in heating energy savings. The MPC strategy demonstrated superior performance over conventional air delivery systems, with electricity consumption reduced by 52-64% and costs lowered by 70-78%. Overall, the implementation of MPC in the radiant floor system proved to be more efficient and effective in maintaining comfort while minimizing energy use compared to traditional HVAC approaches. Traditional HVAC approaches primarily involve forced-air systems that use ductwork to distribute heated or cooled air throughout a building. These systems typically rely on furnaces or air conditioners to regulate indoor temperatures, often using thermostats for control. Additionally, they may include components like fans, filters, and humidifiers.

2.4.6 Other Control Strategies

There are other control strategies such as ratio control, multiloop and multivariable control, adaptive control and sequential logic control.

Ratio control is a specialized form of feedforward control commonly used in the process industries. Its purpose is to maintain a specific ratio between two process variables, which are typically flow rates, one is a manipulated variable, and the other is a disturbance variable. Instead of controlling each variable individually, the focus is on regulating their ratio. This method is often applied in tasks such as setting the correct proportions of components in blending operations, maintaining the stoichiometric ratio of reactants in reactors, controlling the reflux ratio in distillation columns, and optimizing the fuel-air ratio in furnaces (Seborg et al., 2016).

A multivariable control system is designed to handle multiple inputs and outputs simultaneously, typically represented using a matrix of transfer functions between inputs and outputs. It is used to control complex processes where the interaction between different variables can influence system performance. These systems are referred to as multiple-input, multiple-output (MIMO) control systems. These systems can be implemented with centralized or decentralized control strategies to achieve desired performance outcomes (Huilocapi et al., 2019).

In cases where operating conditions or environmental factors change considerably, adaptive control techniques become necessary. Adaptive control systems automatically adjust their parameters to account for unpredictable or unknown variations in the process, unlike gain-scheduling, which is suitable for more predictable situations. Examples of scenarios that may require adaptive control include changes in equipment characteristics, unusual operational statuses like startup or shutdown, large disturbances such as fluctuations in feed composition, ambient variations, shifts in product specifications, and nonlinear behaviors. When such changes can't be easily measured or predicted, adaptive control is typically implemented using a feedback approach, leading to systems often referred to as self-tuning or self-adaptive controllers (Seborg et al., 2016).

Process control strategies are crucial for ensuring stable and efficient operations across various industries. Each strategy has its own advantages: feedback control is simple, feedforward control can manage expected disturbances, and cascade control responds quickly to important disturbances. Adaptive control is notable for its ability to automatically adjust to changing conditions, making it suitable for processes with unpredictable or unknown variations. In order to achieve effective process control, it's important to choose the right strategy based on the specific needs of the process. While traditional methods like feedback and feedforward control are commonly used, advanced techniques like cascade and adaptive control provide significant benefits in more complex or dynamic environments. Selecting the appropriate control strategy is essential for maintaining stable, efficient, and reliable operations.

2.5 Process Modelling: An example of a stirred-tank blending system

Process modeling is a fundamental step in achieving precise real-time process control, as it enables the development of mathematical representations that describe the dynamic behavior of a system. These models help predict process responses to various inputs, optimize control strategies, and improve system stability, ensuring efficient and reliable operation. One of the simplest process control model is the blending system. The blending process is a very common process used in various industries such as chemical, pharmaceutical and food and beverage. Blending process is usually applied to ensure consistency and uniformity in the final product. Ingredients such as additives in food is important to be evenly distributed in the mixture. Similarly, active ingredients must be uniformly distributed to ensure consistent dosage in the medicine.

In this section, the process modelling of a simple stirred-tank blending system is illustrated. The goal of this system is to blend the two inlet streams to produce one outlet stream with the wanted composition by changing the amount of chemical A in the tank. Stream 1 is a mixture of 2 types of chemicals, A and B. Stream 2 only consists of chemical A, hence the mass fraction, $x_2 = 1$. In stream 1, it is assumed that the mass flow rate, w_1 is constant, but the mass fraction of A, x_1 changes with time. In

stream 2, the mass flow rate, w_2 can be altered using the control valve. The mass fraction of chemical A, x is the controlled variable and the value that is desired which is the setpoint is x_{sp} . w_2 is the manipulated variable and x_1 is the disturbance variable (Seborg et al., 2016).

Figure 2.6 shows the illustration of the continuous stirred tank blending system.

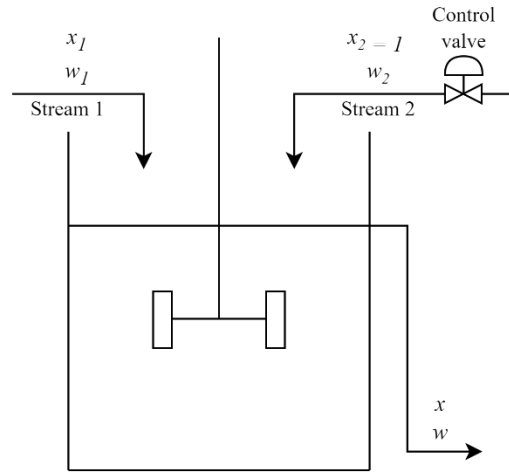


Figure 2.6: Stirred tank blending system

By applying the overall balance and the component A balance to the tank, the following dynamic and steady-state equations are derived:

Overall balance equation:

$$\frac{dm}{dt} = w_1 + w_2 - w \quad (2.1)$$

$$0 = \bar{w}_1 + \bar{w}_2 - \bar{w} \quad (2.2)$$

Component A balance equation:

$$\rho V \frac{dx}{dt} = w_1 x_1 + w_2 x_2 - (w_1 + w_2) x \quad (2.3)$$

$$\rho V \frac{dx}{dt} = f(x, w_1, w_2, x_1) \quad (2.4)$$

$$0 = f(\bar{x}, \bar{w}_1, \bar{w}_2, \bar{x}_1) \quad (2.5)$$

where

Mass fraction of chemical A in stream 1: x_1

Mass flow rate of chemical A in stream 1: w_1

Mass fraction of chemical A in stream 2: $x_2 = 1$

Mass flow rate of stream 2: w_2

Mass fraction of chemical A in output: x

Mass flow rate of output: w

Taylor series is applied to linearize equation (2.3).

$$\rho V \frac{dx}{dt} = f(\bar{x}, \bar{w}_1, \bar{w}_2, \bar{x}_1) + \left. \frac{\partial f}{\partial x} \right|_{ss} (x - \bar{x}) + \left. \frac{\partial f}{\partial w_1} \right|_{ss} (w_1 - \bar{w}_1) + \left. \frac{\partial f}{\partial w_2} \right|_{ss} (w_2 - \bar{w}_2) + \left. \frac{\partial f}{\partial x_1} \right|_{ss} (x_1 - \bar{x}_1) \quad (2.6)$$

$$\rho V \frac{dx'}{dt} = \left. \frac{\partial f}{\partial x} \right|_{ss} x' + \left. \frac{\partial f}{\partial w_1} \right|_{ss} w_1' + \left. \frac{\partial f}{\partial w_2} \right|_{ss} w_2' + \left. \frac{\partial f}{\partial x_1} \right|_{ss} x_1' \quad (2.7)$$

$$\rho V \frac{dx'}{dt} = -\bar{w}_2 x' + (\bar{x}_1 - x)w_1' + (1 - \bar{x})w_2' + \bar{w}_1 x_1' \quad (2.8)$$

Laplace transform is applied to equation (2.8).

$$\rho V s X'(s) = -\bar{w}_2 X'(s) + (\bar{x}_1 - x)W_1'(s) + (1 - \bar{x})W_2'(s) + \bar{w}_1 X_1'(s) \quad (2.9)$$

$$X'(s) = \frac{(\bar{x}_1 - x)W_1'(s)}{\frac{\rho V s}{\bar{w}} + 1} + \frac{(1 - \bar{x})W_2'(s)}{\frac{\rho V s}{\bar{w}} + 1} + \frac{\bar{w}_1 X_1'(s)}{\frac{\rho V s}{\bar{w}} + 1} \quad (2.10)$$

Block diagram is a graphical representation of the control system used to show the flow of information within the system. Each block represents a function or operation, and the quantitative representation of each block is depicted by transfer functions (Seborg et al., 2016). Figure 2.7 shows the block diagram for process dynamics.

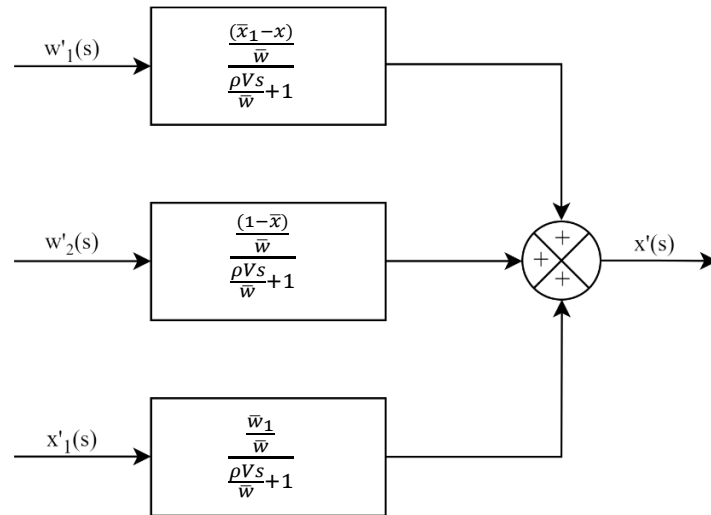


Figure 2.7: Block diagram for process dynamics

Figure 2.8 shows the feedback control block diagram of stirred tank blending system.

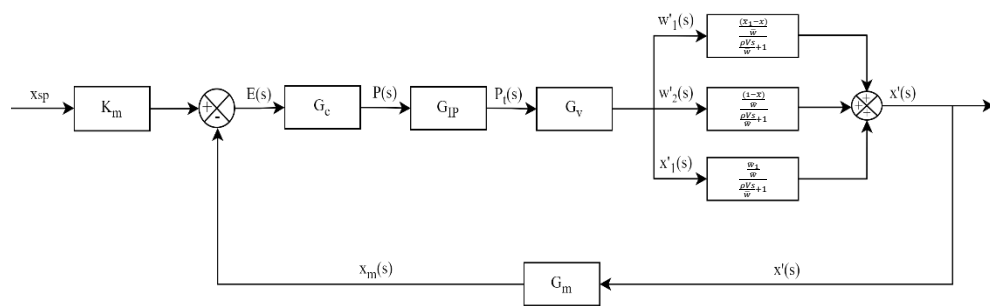


Figure 2.8: Feedback control block diagram of stirred tank blending system

where

K_m = Analyzer calibration

G_c = Feedback controller

G_{IP} = Current-to-pressure transducer

G_v = Control valve

G_p = Stirred tank process

G_m = Analyzer and transmitter (sensor)

The composition of the chemical in the tank is measured by the sensor and the output is sent to the electronic controller. The transfer function of the analyzer and transmitter (sensor), G_m is assumed to obey the first order kinetics, which can be

formulated as $\frac{K_m}{\tau_m s + 1}$. The reading is then compared with the set point and the error signal will be sent to the electronic controller. Assuming a PI controller is used, the transfer function of the controller G_c is $K_C(1 + \frac{1}{\tau_I s})$. Next, the electrical signal will be converted to pneumatic signal by the current-to-pressure transducer, G_{IP} . Since transducers usually have linear characteristics and negligible dynamics, it is assumed that the transducer only consists of a steady-state gain K_{IP} . The output signal of the transducer will be used to adjust the control valve opening, G_v . The transfer function of the control valve is assumed to be $\frac{K_v}{\tau_v s + 1}$. Here, the symbol K represents the steady-state gain whereas τ represents the time constant (Seborg et al., 2016).

A schematic diagram shows the physical connections between the components within the system. Figure 2.9 shows the schematic diagram of the continuous stirred tank blending system. It shows how the mass flow rate w_2 is manipulated to control the tank composition (Seborg et al., 2016).

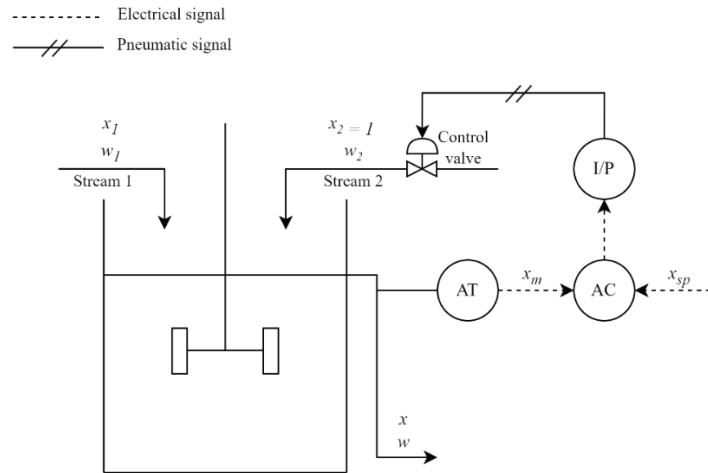


Figure 2.9: Schematic diagram of stirred tank blending system

2.6 Digital Twin

Schluse et al. (2018) explained that a digital twin is a one-to-one virtual replica of a physical asset, such as a machine or a component, that integrates its data, functionality

and communication interfaces. Simulation techniques enable Digital Twins to be brought to life and become experimentable. In the Industry 4.0 era, physical and virtual worlds have to grow together. The study proposes a new structuring element called “Experimentable Digital Twin” that incorporates all relevant components in the virtual system. Digital Twins can provide enhanced simulation that allows testing and optimization of systems in a virtual environment before implementation.

Kazała et al. (2021) presented applicable open-source tools that can be used to create models with the concept of Digital Twins. Developing a Digital Twin necessitates specialized software tools for creating virtual process models, simulations, optimizations, and visualizations. Complex models such as modelling dynamic processes, allowing communication with the environment, and visualising process variables require highly developed softwares. Commercial software packages such as Emulate3D, iTwin, Forge, and Seebo Digital Twin are commonly used in the industry for the development and implementation of Digital Twins. As discussed by VanDerHorn and Mahadevan (2021), Kazała et al. (2021) also further reinforced the idea of Digital Twins consisting of three elements: (i) physical product in real space, (ii) virtual product in a virtual space and set of virtual subsystems, (iii) the connection of data and information that ties the two spaces together. Therefore, a Digital Twin should provide any information that can be obtained from inspecting a physically manufactured product. Mikkili et al. (2015) discussed the advantages of real-time simulation by implementing a model from MATLAB. One of the advantages is time efficiency. It provides more time for engineers to troubleshoot and identify problems at an earlier stage. Besides, testing costs can be reduced, enabling countless simulations without any physical modification. Other than that, it provides more flexibility as it can simulate various real-life scenarios and parameters.

Glatt et al. (2021) states that MATLAB offers an OPC UA library that facilitates universal, bidirectional communication between the simulation model and its real-world counterpart. This means data can flow seamlessly in both directions, allowing for real-time interaction and updates between the digital and physical systems. However, since MATLAB’s simulation environments do not inherently include modules specifically designed for digital twins in material handling, a similar amount

of development and customization work would be required, much like what is needed when using Python-based solutions. Essentially, the creation of the necessary components for a functional Digital Twin demands substantial manual implementation, regardless of the platform used.

Davies et al. (2022) used MATLAB to develop a dashboard as the user interface for the Digital Twin system. The study resulted in a successful development of a dashboard that provided a real-time tracking of component degradation and remaining useful life (RUL) estimations. It allows for effective monitoring and assessment of maintenance strategies, leading to improved planning of maintenance interventions. Additionally, the simulation-based Digital Twin system demonstrates accurate predictions of RUL for critical components, enhancing decision-making in maintenance operations.

Irimia et al. (2019) used Simcenter Amesin software to model and simulate the electric vehicle's control systems, enabling the validation the battery model and analysis of the vehicle under various conditions. The study highlighted that Simcenter Amesin allows efficient Model-in-the-Loop (MIL) simulation, easy modeling of physical models and environments, and provides good reliability and accuracy through its variable step solver with discontinuity handling.

Rodemann and Unger (2018) used SimulationX software to simulate a Modelica based model of a smart building complex. According to the study, Modelica was developed to achieve the purpose of covering a large number of physical domains as a free modeling standard. Many commercial and free tools have been developed using Modelica framework, offering an alternative to MATLAB/Simulink for system modeling and simulation. Modelica framework provides a flexible approach and avoids unidirectional information flow, leading to loops in system design. However, the implementation of more advanced controller approaches in Modelica has certain limitations. More complicated approaches such as Model-Predictive-Control are better suited in high level languages like MATLAB and Python.

Johra et al. (2021) used LabVIEW to model the hydronic heating system with parallel loops. The study aimed to establish a series of digital twins of experimental setups for teaching building physics, energy in buildings, and indoor environmental quality. This looks to enhance e-learning experiences by providing realistic, interactive simulations that allow students to explore complex systems and apply theoretical knowledge in practical scenarios. The study also seeks to address the limitations of physical laboratory access and improve student engagement in engineering education. The LabVIEW model was validated against a reference Modelica model of the same system. The LabVIEW model is better for educational purposes as it provides an interactive graphical user interface that enhances student engagement and understanding. However, the Modelica model serves as a reliable reference for validation, demonstrating high accuracy with strong performance metrics. Therefore, LabVIEW is advantageous for teaching, while Modelica is beneficial for detailed simulations and analysis.

Yang et al. (2020) introduced a novel Digital Twin simulation platform for multi-rotor UAV by combining Unity, ROS, MATLAB and SimulIDE. MATLAB can conduct method verification using the toolboxes provided. Unity and MATLAB were combined to present a digital twin theory verification platform. MATLAB enables processing, predicting, and learning the interactive data between the twin and physical platform by using the data processing tools provided. Unity will then use the processed results to adjust the parameters of the physical model. Due to MATLAB being a lower level programming language, causing a gap between data byte alignment and C# language. Hence, Unity and MATLAB cannot be directly connected. As MATLAB supports interaction with C++ language, it is used as a communication interface between MATLAB and unity. As MATLAB does not allow multi-threading, hence multi-threading was not used to realize real-time data transmission and reception in this study.

Table 2.1 provides a comparative summary of various modelling software, including Emulate3D, iTwin, Forge, Seebo, MATLAB Simulink, Simcenter Amesim, SimulationX Modelica, LabVIEW, and Unity.

Table 2.1: Summary of different modelling softwares

Software	Characteristics
Emulate3D, iTwin, Forge, and Seebo	<ul style="list-style-type: none"> - Commercial software packages - Meant for complex models that require highly developed software
MATLAB Simulink	<ul style="list-style-type: none"> - Offers an Open Platform Communications Unified Architecture (OPC UA) library - Allows effective monitoring and assessment of maintenance strategies - Able to handle more advanced controller approaches - Supports interaction with C++ programming language - Does not allow multi-threading - Enables processing, predicting and learning interactive data
Simcenter Amesin	<ul style="list-style-type: none"> - Allows efficient Model-in-the-Loop (MIL) simulation - Easy modeling of physical models and environments - Provides good reliability and accuracy
SimulationX Modelica	<ul style="list-style-type: none"> - covers many physical domains as a free modeling standard - provides a flexible approach and avoids unidirectional information flow - Better accuracy compared to LabVIEW - Less suitable to handle more advanced controller approaches
LabVIEW	<ul style="list-style-type: none"> - Provides an interactive graphical user interface - Not suitable for detailed simulation and analysis
Unity	<ul style="list-style-type: none"> - Higher level C# programming language - Adjusts parameters of physical model based on processed results

MATLAB Simulink stands out as a powerful and versatile tool for developing Digital Twin systems, particularly in engineering and industrial applications. It offers robust simulation capabilities, advanced data processing tools, and strong

communication support. Unlike Emulate3D, iTwin, Forge, and Seebo which are commercial platforms designed for highly complex models that require significant investment, MATLAB provides a more flexible and accessible environment without sacrificing functionality. The integration of the OPC UA library enables seamless, bidirectional communication between the virtual model and the physical system, facilitating real-time interaction and monitoring. While Simcenter Amesim excels in physical modelling and reliability, MATLAB offers a broader range of advanced controller design tools and superior data analytics capabilities. Compared to SimulationX and Modelica, which are strong in multi-domain physical modelling but limited in advanced control strategies, MATLAB supports complex algorithm development and predictive control. LabVIEW, though useful for educational purposes due to its interactive graphical interface, lacks the depth required for detailed simulation and real-time data analysis. Similarly, while Unity excels in 3D visualisation and interactivity, it does not match MATLAB's analytical and simulation strength. Overall, MATLAB provides the ideal balance of modelling, control, prediction, and integration, making it the preferred platform for those seeking a technically robust and comprehensive solution for Digital Twin development.

CHAPTER 3

METHODOLOGY

3.1 Introduction

This chapter explains the method of conducting this study to achieve the aims and objectives. Section 3.2 shows the flow chart of the project. Section 3.3 is the process description, section 3.4 focuses on the experiment using physical equipment and section 3.5 focuses on development and simulation of the digital twin that mirrors the physical equipment.

3.2 Project Flow

Figure 3.1 is the flow chart of this project.

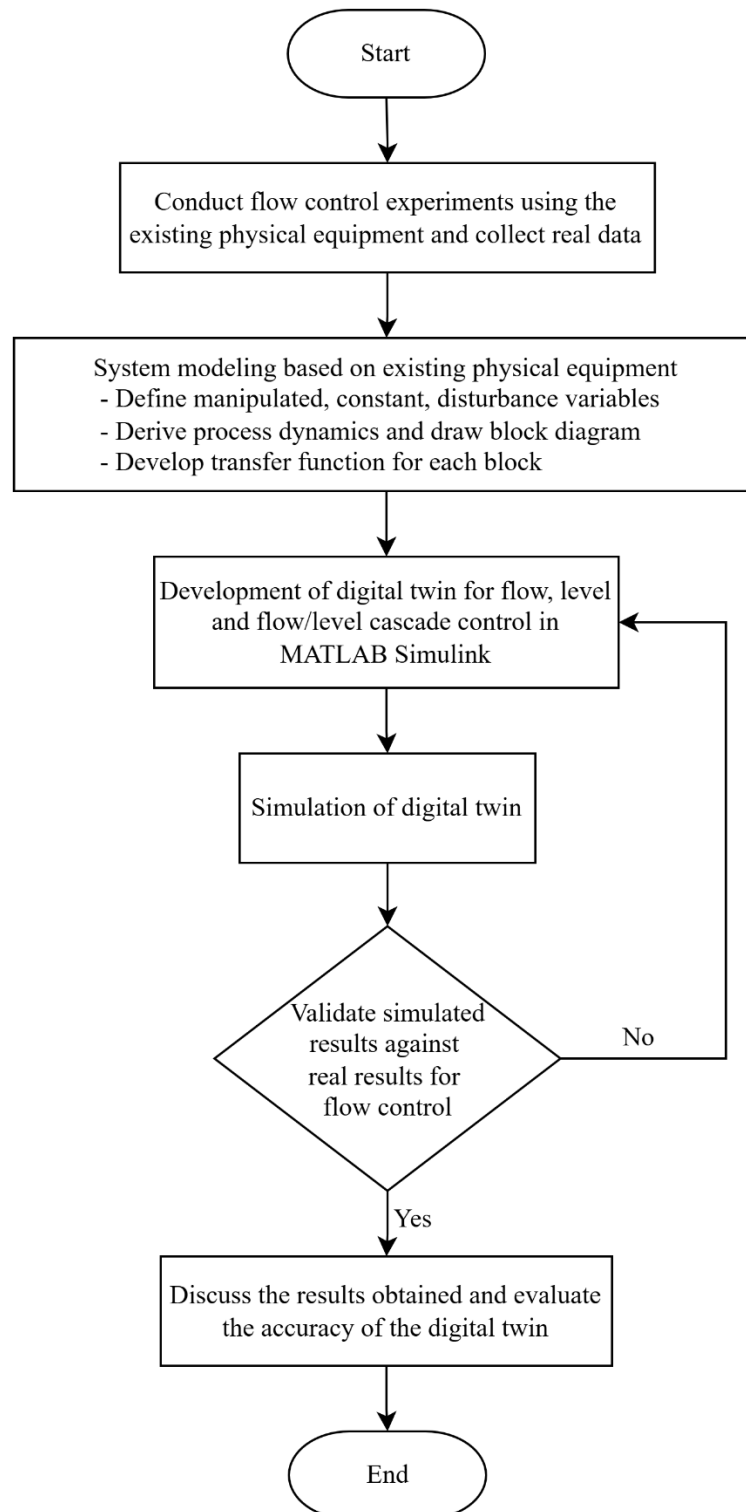


Figure 3.1: Project flow chart

3.3 Process Description

The schematic diagram of the flow and level control system to be modelled in this study is shown in Figure 3.2. This system is denoted as the Flow/Level Cascade Control Trainer (Model: SE 465), which involves the pumping of water from sump tank, T-601 by P-601 to the level tank, T-602, then return to sump tank, T-601 by gravity flow. A water rotameter and flow transmitter, FI-602 and FT-602 respectively are used to measure the water flow rate. A differential pressure transmitter, LT-601 is used to measure the water level in T-602 by using differential pressure. In this process, the ultimate goal is to control the water level in T-602. To achieve this, PID controllers LIC-601 and FIC-602 are used to control water level and water flow respectively. The control strategies includes feedback flow control, feedback level control, and flow/level cascade control model.

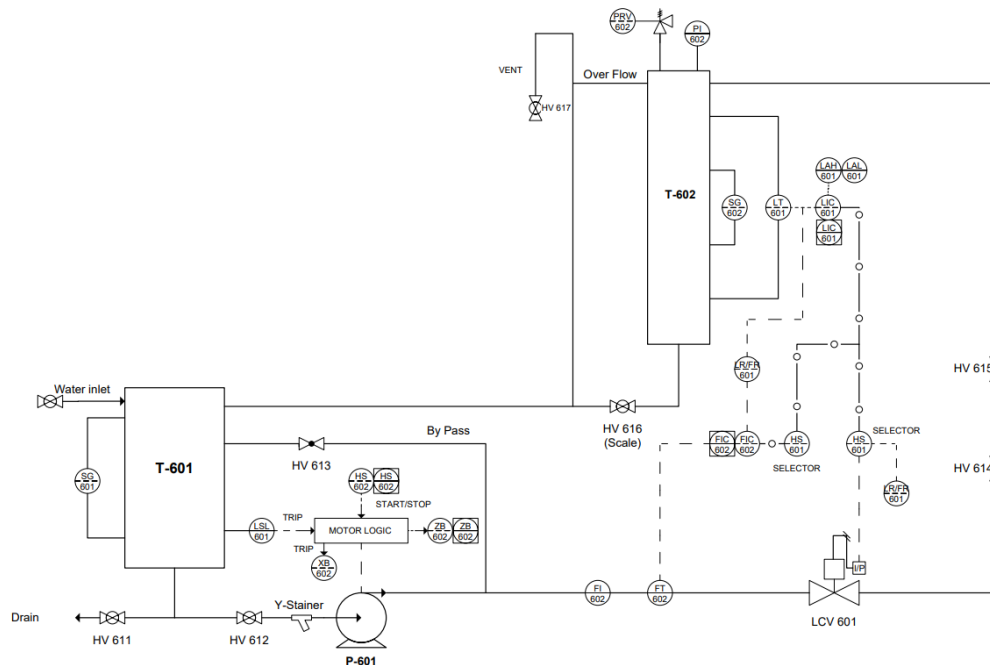


Figure 3.2: Schematic diagram of SOLTEQ® flow/level cascade control trainer (model: SE 465)

Table 3.1 shows the main instruments used in the flow/level cascade control trainer and their functions.

Table 3.1 Instruments functions

No.	Instrument	Tag No.	Description	Range
1	PID Controller	LIC-601 FIC-602	Microprocessor based PID controller, controlling level/flow	-
2	Recorder	LR-601 FR-601	Paperless chart recorder	-
3	Water Flow Transmitter	FT-602	Primary flow measurement device giving 4-20mA output	0 – 20 LPM
4	D/P Transmitter	LT-601	Level measurement using differential pressure	0 – 1000 mmH ₂ O
5	Control Valve	LCV-601	½ inch globe type valve with Cv=2.5, linear characteristic with I/P positioner and I/P converter	1 - 100%
6	Pumps	P-601	Water circulation pumps	0 – 20 LPM
7	Process Tanks	T-601 T-602	Sump Tank Level Control Tank	60 L 20 L
8	Relief Valve	PSV-602	Mechanically activated device, spring loaded normally closed valve. Opens and purges air to atmosphere in case of over pressure in tank	-
9	Rotameter	FI-602	Flowrate measurement for water	0 – 20 LPM
10	Pressure Indicator	PI-602	Dial gauge pressure indicator at location	0 – 3000 mmH ₂ O
11	Side Glass	SG-601 SG-602	Observation of water level in tanks	-

3.4 Experimental Methods

In this project, only flow control experiment will be conducted. The local control panel allows the selection of any one of the experiments. The flow control loop involves the water flow transmitter FT-602 to feed the signal to the controller FIC-602 that will control the valve LCV-601. Similarly, the level control loop involves the D/P transmitter LT-601 to feed the signal to the controller LIC-601 that will control the valve LCV-601. In the flow/level cascade control loop, the D/P transmitter LT-601 will feed the signal to the controller LIC-601. The output of the controller will then be used as the set point for the controller FIC-602. The flow rate measurement from the water flow transmitter FT-602 will be compared with the set point and the controller will control the valve LCV-601.

The flow control experiment begins with the general start-up steps, ensuring all valves are set to their initial positions according to the flow control settings. The experiment is initiated by selecting the "Flow Control" mode. In "Manual" mode, the proportional band (PB), integral (I), and derivative (D) values are entered, with initial values set at $PB = 30\%$, $I = 0 \text{ s}^{-1}$, and $D = 0 \text{ s}$ for flow control. The output is gradually adjusted until the flow measurement stabilises at 10 LPM. Subsequently, the mode is switched to "Auto," and the set point is changed to 15 LPM. This is repeated for different values of PB, specifically 150%, 300%, 500%, and 900%. In the second iteration of the experiment, the value of PB is held constant at 150%, while D remains at 0 s, and the value of I is varied to 5 s^{-1} , 20 s^{-1} , 50 s^{-1} , 80 s^{-1} , and 100 s^{-1} . The third iteration involves keeping PB constant at 150% and I at 20 s, while D is adjusted to 2 s, 3 s, 5 s, 7 s, 10 s, and 50 s. During each experiment, the response of the manipulated variable, the output flow rate, is observed and recorded in terms of oscillation period, amplitude, and the time taken to reach steady-state conditions. It should be noted that the relationship between the proportional band and proportional controller is $PB = \frac{100\%}{P}$.

3.5 Modelling and Simulation

This project focuses on flow control, level control, and flow/level cascade control systems. The process of modelling the digital twin begins with deriving the process dynamics for each of these control systems. The initial step involves determining the transfer function for each instrument and level tank process, which includes modelling and linearising any non-linear processes using the Laplace transform. Once the transfer functions are derived, they are incorporated into the respective block diagrams. These block diagrams for flow control, level control, and flow/level cascade control are then constructed using MATLAB Simulink software to simulate the system dynamics. All transfer functions are entered into the blocks in MATLAB Simulink to replicate the behaviour of their real-life counterparts. This includes constants, steady-state gains, time constants and PID controller values. Then, each component of the model are simulated individually first to minimise troubleshooting issues when the entire model is integrated. Subsequently, simulations of the entire control loop are conducted, and the output displayed on the scope will be compared and validated against the results from the real-life experiment.

CHAPTER 4

RESULTS AND DISCUSSION

4.1 Flow Control Experiment

This section presents a detailed discussion of the real-time experimental results for the flow control system. In this system, the flow rate serves as the controlled variable, while the valve opening acts as the manipulated variable. The valve opening is adjusted through a feedback control strategy to maintain the desired flow rate.

4.1.1 Proportional Controller

Figure 4.1 shows the response of flow rate toward the set point change at different proportional band (PB) values, while using only the proportional controller. The relationship of the proportional gain (P) and the proportional band is $PB = \frac{100\%}{P}$, which implies that a higher value of PB indicates a lower proportional gain.

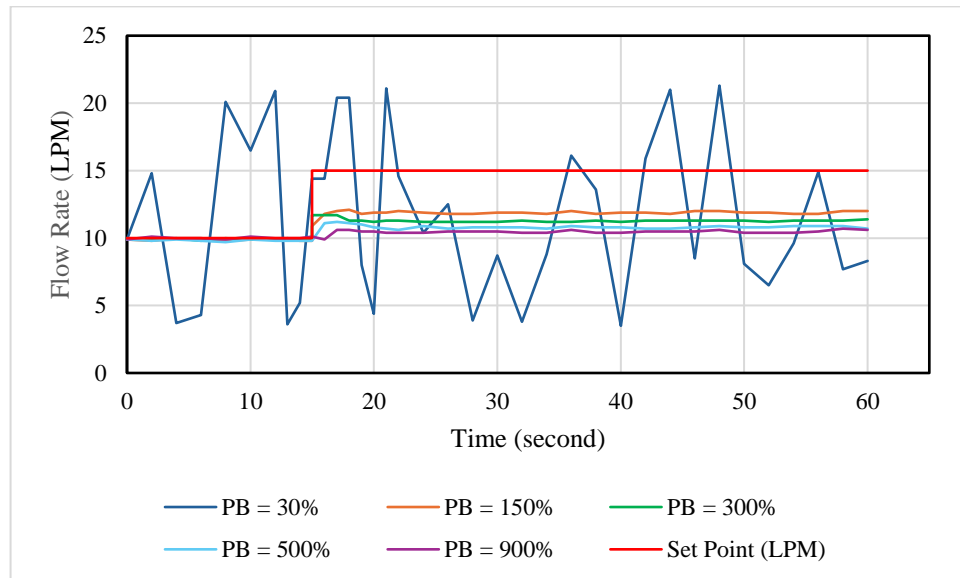


Figure 4.1: Response of flow rate (controlled variable) toward the set point change (from 10 LPM to 15 LPM) regulated by proportional controller with different PB values

Figure 4.1 illustrates how varying Proportional Band (PB) settings of a proportional controller affect its ability to regulate flow rate (in litres per minute, LPM) over time (in seconds) after a step change in the set point of the flow rate. In this figure, each curve corresponds to a different PB value: 30%, 150%, 300%, 500%, and 900%, which equate to proportional gains of $P = 3.33, 0.67, 0.33, 0.20$, and 0.11 , respectively. The red line indicates the setpoint change from 10 LPM to 15 LPM at $t = 15$ seconds. Lower PB values (higher proportional gain), such as 30% (dark blue colour graph in Figure 4.1), result in faster system responses but cause significant fluctuations and oscillations. This indicates instability due to overly aggressive control, making the system highly sensitive to the deviation of the controlled variable from its set point value. As the PB value increases (proportional gain decreases), the system exhibits improved stability with reduced oscillations. However, this comes at the cost of a larger offset between the output flow rate and the setpoint, as well as a slower response. For instance, the offset between the actually stabilized value of the flowrate and the set point is 3 LPM for PB setting of 150%. However, the offset increases to 4.5 LPM under a PB setting of 900%. This observation highlights that a proportional controller yield quicker responses and lower offset towards a step change in the set point if PB value is lower (proportional gain is higher) but there is a risk of instability in the response. On the other hand, with a higher PB value (or a lower proportional gain),

stability can be enhanced at the expense of slower regulation and increased offset. The most significant drawback of proportional controller is the occurrence of offset which causes the controlled variable to be always deviated from the desired set point.

4.1.2 Integrative Controller

Figure 4.2 illustrates the response of the flow rate (controlled variable) to a step change in the setpoint from 10 LPM to 15 LPM, as regulated by a PI controller. The Proportional Band (PB) is held constant at 150%, corresponding to a proportional gain (P) of 0.67.

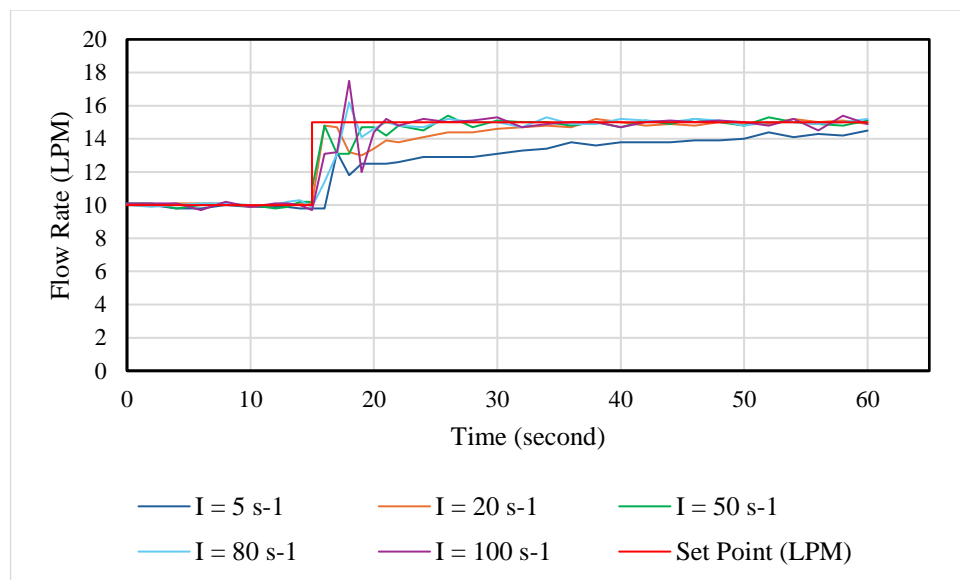


Figure 4.2: Response of flow rate (controlled variable) toward the set point change (from 10 LPM to 15 LPM) regulated by the proportional controller and integral controller with different I values and constant PB = 150%

Each curve in Figure 4.2 represents the response of the flow rate toward the set point change controlled by PI controller with different integral gain setting: 5 s^{-1} , 20 s^{-1} , 50 s^{-1} , 80 s^{-1} , and 100 s^{-1} . The integral gain is the reciprocal of integral time, τ_I , which means $I = \frac{1}{\tau_I}$. Besides, the red line indicates the setpoint change from 10 LPM to 15 LPM which occurs at $t = 15 \text{ s}$. With the incorporation of the integral action in the

controller, the offset between the controller variable and the desired set point in the proportional control loop is generally eliminated, as the controlled variable can achieve the desired set point after given sufficient time. Since the integral function is inversely proportional to the response, the PI controller with I of 5 s^{-1} (higher integral time τ_I at 0.2 s), result in a slower and more gradual response, taking longer to reach steady state. As the integral gain increases to 80 s^{-1} or 100 s^{-1} (integral time τ_I decreases to 0.0125 s and 0.01 s), the system responds more quickly and achieves steady state faster. This quicker reaction comes at the cost of increased instability and overshoot, indicating that overly aggressive integral action makes the system more sensitive to step change in the set point. This observation highlights the trade-off between responsiveness and stability. Lower integral gain result in smaller or no overshoots but slower convergence to the setpoint. In contrast, higher integral gain allow the system to respond more rapidly, but this comes with initial instability and significant overshoot.

4.1.3 Derivative Controller

Figure 4.3 shows the response of the flow rate to a change in the setpoint at different derivative (D) values, with the Proportional Band (PB) fixed at 150%, corresponding to a proportional gain (P) of 0.67, and the integral gain (I), which is the reciprocal of the integral time, is set to 20 s^{-1} .

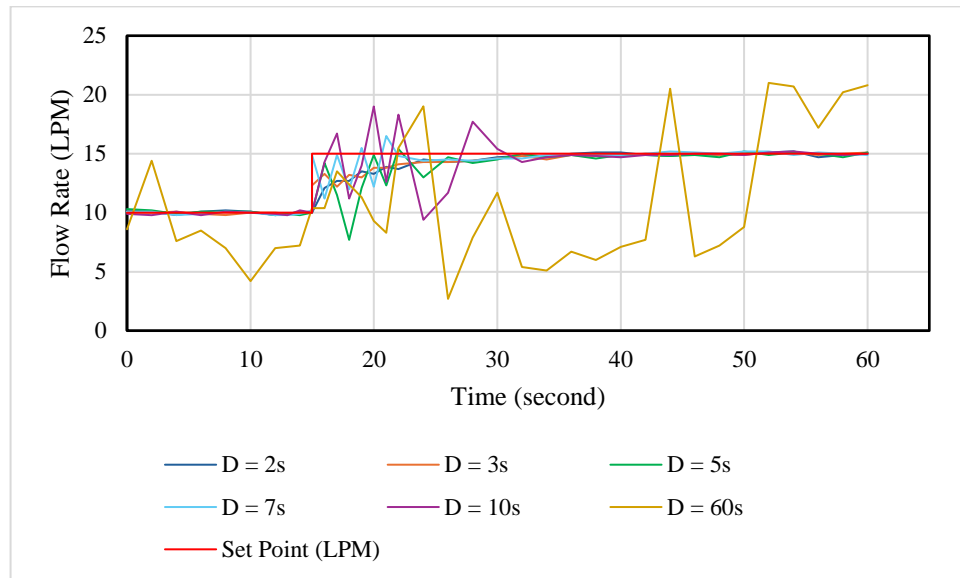


Figure 4.3: Response of flow rate (controlled variable) toward the set point change (from 10 LPM to 15 LPM) regulated by proportional, integral, and derivative controller with different D Values, constant $PB = 150\%$ and $I = 20 \text{ s}^{-1}$

Each curve in Figure 4.3 represents the response of flow rate toward the set point change controlled by a PID controller with different derivative time setting: 2 s, 3 s, 5 s, 7 s, 10 s, and 60 s. The red line indicates the setpoint change from 10 LPM to 15 LPM which occurs at $t = 15 \text{ s}$. In general, the incorporation of the derivative action into the controller has caused the response to be faster and less sluggish, as compared to the performance demonstrated by PI controller in Figure 4.2. For instance, with the relatively shorter derivative times, such as $D = 2 \text{ s}$, 3 s , and 5 s , the results show a relatively smooth response with minimal oscillations, allowing the system to approach the setpoint efficiently and stably. These settings help dampen sudden changes without overly delaying the system's response, achieving a good balance between responsiveness and stability. As the derivative time increases at $D = 7 \text{ s}$, the system begins to show signs of instability, with noticeable fluctuations around the setpoint during the transient phase. For the extreme case with very high D value (60 s), the response toward the set point change becomes highly unstable, as the output exhibits excessive oscillations. This instability is due to overly aggressive derivative action, making the system overly sensitive to any changes occur in the system. In short, this observation highlights the trade-off involved in tuning derivative settings, in which the lower derivative times provide more stable and well-damped responses, eliminating

overshoots, while excessively high derivative times lead to large amount of oscillations and unstable behaviour.

4.2 Process Modelling

This section presents the modelling process of the control system in detail. The process begins with a description of the individual instruments and components involved. These elements are then interconnected to form a closed feedback control loop, with the corresponding mathematical relationships also defined. The control loops considered in this modelling are: (i) the flow control system, (ii) the level control system, and (iii) the cascade control system.

4.2.1 Modelling of Process and Instruments

In this subsection, the mathematical modelling of the liquid level dynamics in the tank, along with the relevant instruments such as the transducer, control valve, and transmitter is described in detail. The modelling involves formulating dynamic ordinary differential equations (ODEs) that represent the behaviour of the process or instruments. These equations are subsequently transformed into transfer functions using the Laplace transform, enabling simulation in Simulink software.

4.2.1.1 Level Tank

A level tank is a vessel used to store and control the level of liquid within it. It features an inlet for liquid flow, an outlet for discharge, and a level measurement device (sensor) to monitor the liquid level. The level is maintained through a control system that adjusts the flow rate at the inlet based on feedback from the level measurement. In the

level tank employed in this study, the outlet flow rate is not regulated and it is dependent on the liquid level in the level tank. To mathematically model the dynamical behaviour of the level tank, mass conservation (or mass balance) is applied to relate the inflow, q_i , the outflow, q , and the water level, h within the level tank. Here, the difference between the inflow and outflow equals to the accumulation of the liquid (or rate of change of liquid volume) in the level tank, $A \frac{dh}{dt}$ is formulated by the following equation:

$$A \frac{dh}{dt} = q_i - q \quad (4.1)$$

where A = area of level tank

h = height of liquid in the level tank

q_i = input stream

q = output stream

If the inflow rate is higher than the outflow rate, the water level increases, while if the outflow exceeds the inflow, the water level decreases. When the inflow and outflow are equal, the water level remains stable, ensuring a steady-state condition within the system. Since the outflow is driven by gravity and not actively controlled, the outlet flow rate can be expressed as a function of the liquid level in the tank, as given by (Seborg et al., 2016):

$$q = C_v \sqrt{h} \quad (4.2)$$

where C_v is valve flow coefficient, a constant that depends on the opening of the valve. By inserting equation (4.2) into equation (4.1), the following equation is resulted:

$$A \frac{dh}{dt} = q_i - C_v \sqrt{h} \quad (4.3)$$

The C_v from Eq. (4.2) can be formulated as (Seborg et al., 2016):

$$C_v = \frac{q}{N_f(l) \frac{\Delta p_v}{g_s}} \quad (4.4)$$

where $N = \text{conversion unit } \frac{gpm}{psi^{\frac{1}{2}}}$

$f(l) = 1\% \text{ to } 100\% \text{ valve opening}$

$\Delta p_v = \text{pressure drop across valve}$

$g_s = \text{specific gravity of water} = 1$

Under the steady-state condition, the height of liquid in the level tank is not changing with respect to time. Thus, $A \frac{dh}{dt} = 0$, and equation (4.3) can be transformed to:

$$0 = \bar{q}_i - C_v \sqrt{\bar{h}} \quad (4.5)$$

where \bar{q}_i and \bar{h} are input stream flow rate and height of liquid in the level tank under the steady-state condition, respectively.

Since the process is non-linear (due to \sqrt{h} term), linearization by using Taylor series approximation is required to convert the mathematical equations that describe this process to a linear transfer function. To do this, let:

$$A \frac{dh}{dt} = f(q_i, h) = q_i - C_v \sqrt{h} \quad (4.6)$$

$$0 = f(\bar{q}_i, \bar{h}) \quad (4.7)$$

and the Taylor series approximation can be written as:

$$f(q_i, h) \approx f(\bar{q}_i, \bar{h}) + \left. \frac{\partial f}{\partial q_i} \right|_{\bar{q}_i, \bar{h}} (q_i - \bar{q}_i) + \left. \frac{\partial f}{\partial h} \right|_{\bar{q}_i, \bar{h}} (h - \bar{h}) \quad (4.8)$$

The difference between the dynamic and steady state variables is denoted as the deviation variable, which is given by:

$$q_i - \bar{q}_i = q'_i \quad (4.9)$$

$$h - \bar{h} = h' \quad (4.10)$$

Substitute equation (4.9) and (4.10) into equation (4.8),

$$f(q_i, h) - f(\bar{q}_i, \bar{h}) = \left. \frac{\partial f}{\partial q_i} \right|_{\bar{q}_i, \bar{h}} q'_i + \left. \frac{\partial f}{\partial h} \right|_{\bar{q}_i, \bar{h}} h' \quad (4.11)$$

By differentiating equation (4.6) with respect to q_i and h , the following expressions yield:

$$\left. \frac{\partial f}{\partial q_i} \right|_{\bar{q}_i, \bar{h}} = \frac{\partial f}{\partial q_i} (\bar{q}_i - C_v \sqrt{\bar{h}}) = 1 \quad (4.12)$$

$$\left. \frac{\partial f}{\partial h} \right|_{\bar{q}_i, \bar{h}} = \frac{\partial f}{\partial h} (\bar{q}_i - C_v \sqrt{\bar{h}}) = -\frac{C_v}{2\sqrt{\bar{h}}} \quad (4.13)$$

Substitute equations (4.12) and (4.13) into equation (4.11),

$$A \frac{dh'}{dt} = q'_i - \frac{C_v}{2\sqrt{\bar{h}}} h' \quad (4.14)$$

To obtain the transfer function of this process, Laplace transform is applied to equation (4.14), which gives:

$$AsH'(s) = Q'_i(s) - \frac{C_v}{2\sqrt{\bar{h}}} H'(s) \quad (4.15)$$

After algebraic rearrangement of equation (4.15), the following transfer function is obtained:

$$G_p = \frac{H'(s)}{Q'_i(s)} = \frac{\frac{2\sqrt{\bar{h}}}{C_v}}{\left[\frac{2\sqrt{\bar{h}}}{C_v} As + 1 \right]} \quad (4.16)$$

It should be noted that Equation (4.16) is depicting the change of the height of liquid in level tank due to the change of the inlet flow rate of the liquid to the tank. Furthermore, it is in the form of first order transfer function $\frac{K_p}{\tau_p s + 1}$, in which the corresponding gain and time constant are given by:

$$K_p = \frac{2\sqrt{\bar{h}}}{C_v} \quad (4.17)$$

$$\tau_p = \frac{2\sqrt{h}}{c_v} A \quad (4.18)$$

4.2.1.2 Control Valve and I/P Transducer

The current-to-pressure transducer plays a role in converting electrical signals into pressure, which is then used to control the operation of the control valve. Due to the relatively fast response (almost immediate response) of the I/P transducer as compared to the entire process, it is reasonable to assume the transducer has negligible dynamic effects with time constant of zero in the transfer function that depicts its dynamical behaviour (Seborg et al., 2016). As a result, the system's behaviour is defined solely by the transducer's gain, denoted as K_{IP} , which represents the proportional relationship between the input and output:

$$G_{IP} = K_{IP} \quad (4.19)$$

The control valve receives pressure signals from the transducer and adjusts its opening in % to regulate the flow rate in LPM. However, its response is not immediate as mechanical and fluid dynamic factors introduce a delay. This delay helps maintain system stability by preventing abrupt changes that could lead to oscillations. As a result, its time constant, τ_v , in the transfer function that describes its dynamics is not negligible, and it represents the time scale required for the valve to respond after a change in input. Thus, the transfer function of the control valve is given by:

$$G_v = \frac{K_v}{\tau_v s + 1} \quad (4.20)$$

where K_v = control valve gain

τ_v = control valve time constant

4.2.1.3 Transmitter

The main function of a flow transmitter is to measure the flow rate and transmit it as an electronic signal to the controller. It is reasonable to assume the flow transmitter has linear characteristics and negligible dynamics (where the time constant is zero in the transfer function) due to its significantly fast response as compared to the other processes in the control system to be studied (Seborg et al., 2016). Therefore, the transfer function of the flow transmitter is given by:

$$G_m = K_m \quad (4.21)$$

where K_m = flow transmitter gain.

The level transmitter measures the height difference and transmits it as an electronic signal to the controller. Similar to the flow transmitter, it is also reasonable to assume that the level transmitter has linear characteristics and negligible dynamic effects with zero time constant in its transfer function (Seborg et al., 2016). Thus, the transfer function of the level transmitter is given by:

$$G_l = K_l \quad (4.22)$$

where K_l = level transmitter gain.

4.2.1.4 PID Controller

In a feedback control loop, the controller receives an input signal from sensors, representing the measured process variable. It then compares this value with the setpoint and determines the necessary corrective action. The controller transmits this adjustment as an electrical signal to the transducer, which converts it into pressure to regulate the control valve for system that is controlling/manipulating the flow rate of

a fluid. This continuous process ensures the system maintains stability and responds effectively to changes or disturbances. The ideal PID controller has an equation of:

$$G_c = K_c[1 + \frac{1}{\tau_I s} + \tau_D s] \quad (4.23)$$

where K_c = controller gain

τ_I = time constant of I controller

τ_D = time constant of D controller

In equation (4.23), it has been assumed that the proportional (P), integral (I) and derivative (D) controllers are connected in parallel manner.

In addition, a derivative filter, N is used in the PID controller to reduce the sensitivity of control calculations to noisy measurements under the actual scenario. Noisy measurements refer to high-frequency components or random fluctuations in the process. The ideal form of the derivative action, $K_c \tau_D s$ can amplify noise unless the measurement is properly filtered. With the incorporation of the derivative filter, the transfer function of the PID controller becomes:

$$G_c = K_c + \frac{K_c}{\tau_I s} + K_c \tau_D \frac{\frac{1}{\alpha \tau_D}}{1 + \frac{1}{\alpha \tau_D s}} \quad (4.24)$$

where $N = \frac{1}{\alpha \tau_D}$ and α = a constant between 0.05 and 0.2, with 0.1 being a common choice (Seborg et al., 2016).

The equation of a parallel PID controller in Simulink software is given in the following form:

$$G_c = P + I \frac{1}{s} + D \frac{N}{1 + N \frac{1}{s}} \quad (4.25)$$

By comparing equation (4.24) and (4.25), it can be deduced that the P , I , D and N settings to be inserted to the Simulink software during the simulation is given by:

$$P = K_c, I = \frac{K_c}{\tau_I}, D = K_c \tau_D, \text{ and } N = \frac{1}{\alpha \tau_D}.$$

4.2.2 Control Loop

This subsection explains how the previously described processes and instruments are interconnected to form various control systems. The control systems modelled include: (i) a feedback flow control system, (ii) a feedback level control system, and (iii) a cascade control system. For each system, the equations relating the control variables to changes in the setpoint are formulated

4.2.2.1 Flow Control Loop

Figure 4.4 illustrates the flow control feedback loop modelled and to be simulated by Simulink software. The dynamic relationship between the output water flow rate and the step input in Figure 4.4 can be characterized by a single transfer function, in which the detailed derivation is shown in the following text.

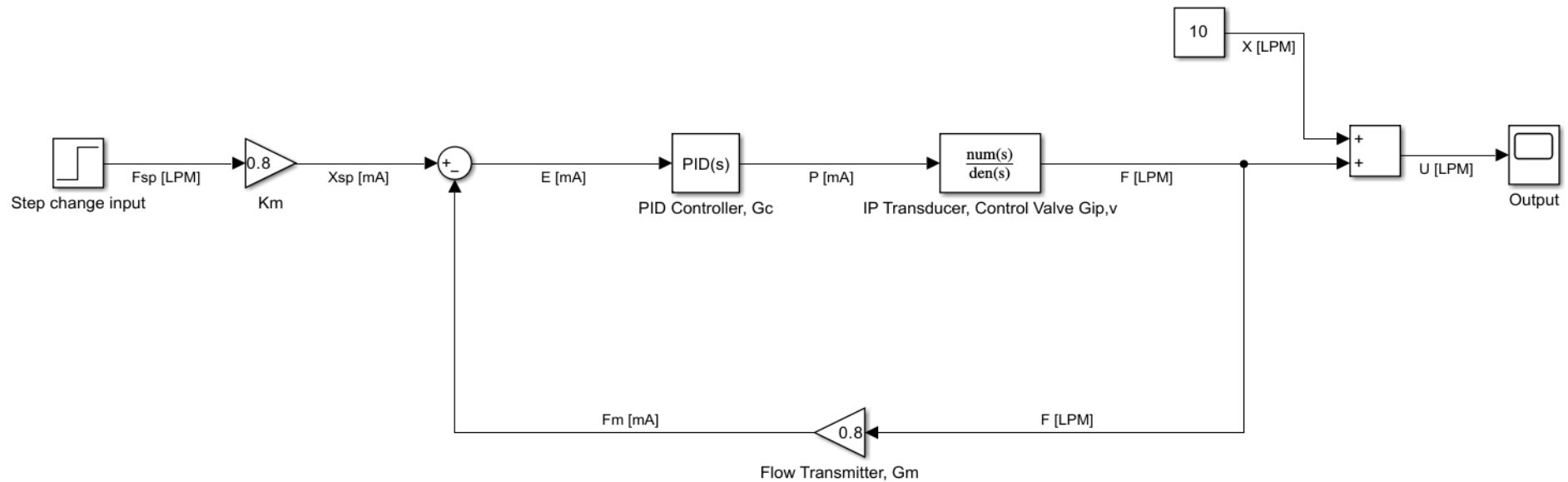


Figure 4.4: Flow control feedback loop in MATLAB Simulink

From Figure 4.4, the following equations can be derived:

$$F = G_{IP,v}P \quad (4.26)$$

$$P = G_c E \quad (4.27)$$

$$E = X_{sp} - F_m \quad (4.28)$$

Substituting equation (4.28) into equation (4.27) gives:

$$P = G_c(X_{sp} - F_m) \quad (4.29)$$

Substituting equation (4.29) into equation (4.26) gives:

$$F = G_{IP,v}G_c(X_{sp} - F_m) \quad (4.30)$$

In addition, the following relations can be formulated according to Figure 4.4:

$$X_{sp} = K_m F_{sp} \quad (4.31)$$

$$F_m = G_m F \quad (4.32)$$

Substituting equation (4.31) and equation (4.32) into equation (4.30) gives:

$$F = G_{IP,v}G_c(K_m F_{sp} - G_m F) \quad (4.33)$$

$$\frac{F}{F_{sp}} = \frac{G_{IP,v}G_c K_m}{G_{IP,v}G_c G_m + 1} \quad (4.34)$$

The block diagram in Figure 4.4 indicates that the step change input is a deviational value. However, the real-time output flow rate, U includes a bias term (10 LPM) to represent the actual flow rather than just the deviation. Therefore, a bias, X is added to the output flow rate, F as shown in equation (4.35).

$$U = F + X \quad (4.35)$$

$$U = \frac{G_{IP,v}G_c K_m F_{sp}}{G_{IP,v}G_c G_m + 1} + X \quad (4.36)$$

4.2.2.2 Level Control Loop

Figure 4.5 shows level control feedback loop modelled and to be simulated by Simulink software. The dynamic relationship between the output water level and the step input in Figure 4.5 can be characterized by a single transfer function. The unit conversion blocks are ignored in the derivation of the overall transfer function.

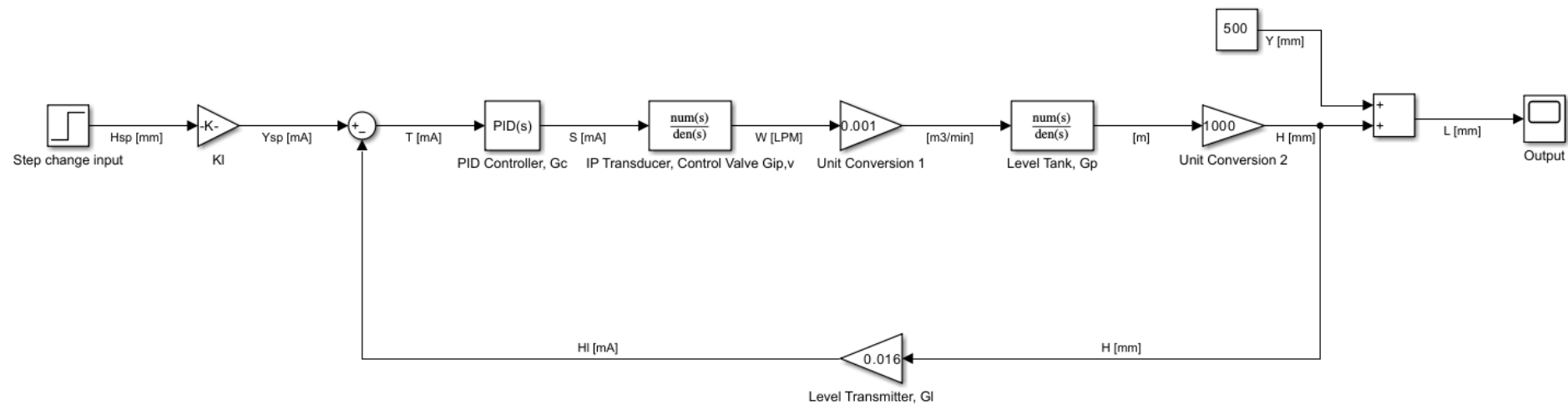


Figure 4.5: Level control feedback loop in MATLAB Simulink

According to Figure 4.5, the following equations can be written:

$$H = G_p W \quad (4.37)$$

$$W = G_{IP,v} S \quad (4.38)$$

$$S = G_c T \quad (4.39)$$

$$T = Y_{sp} - H_l \quad (4.40)$$

Substituting equation (4.40) into equation (4.39) gives:

$$S = G_c (Y_{sp} - H_l) \quad (4.41)$$

Substituting equation (4.41) into equation (4.38) gives:

$$W = G_{IP,v} G_c (Y_{sp} - H_l) \quad (4.42)$$

In addition, the following relations can be formulated according to Figure 4.5:

$$Y_{sp} = K_l H_{sp} \quad (4.43)$$

$$H_l = G_l H \quad (4.44)$$

Substituting equation (4.43) and equation (4.44) into equation (4.42) gives:

$$W = G_{IP,v} G_c (K_l H_{sp} - G_l H) \quad (4.45)$$

Substituting equation (4.45) into equation (4.37) gives:

$$H = G_p G_{IP,v} G_c (K_l H_{sp} - G_l H) \quad (4.46)$$

$$\frac{H}{H_{sp}} = \frac{G_p G_{IP,v} G_c K_l}{G_p G_{IP,v} G_c G_l + 1} \quad (4.47)$$

The block diagram in Figure 4.5 indicates that the step change input is a deviational value. However, the real-time output water level, L includes a bias term (250 mm) to represent the actual flow rather than just the deviation.

Therefore, a bias, Y is added to the output flow rate, H as shown in equation (4.48).

$$L = H + Y \quad (4.48)$$

$$L = \frac{G_p G_{IP,v} G_c K_l H_{Sp}}{G_p G_{IP,v} G_c G_l + 1} + Y \quad (4.49)$$

4.2.2.3 Flow/Level Cascade Control Loop

Figure 4.6 illustrates the flow/level cascade control loop to be modelled and simulated by Simulink software. The level control system serves as the primary loop and the flow control system serves as the secondary loop. The inner loop is responsible for detecting and responding to flow disturbances, while the outer loop regulates and maintains the water level in the tank. The dynamic relationship between the output water level and the step input of the flow/cascade control loop in Figure 4.6 can be characterized by a single transfer function. The unit conversion blocks are ignored in the derivation of the overall transfer function.

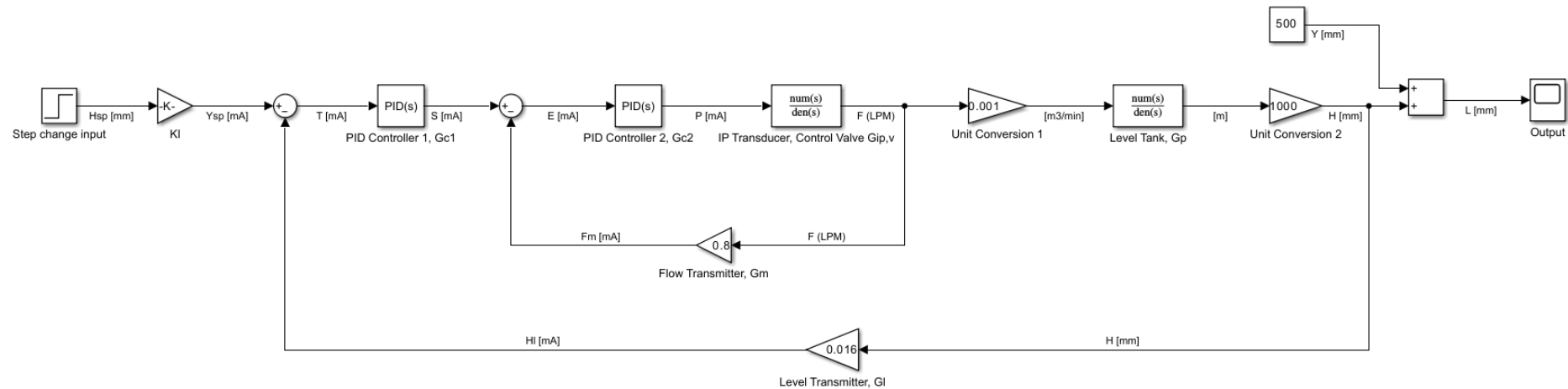


Figure 4.6: Flow/level cascade control loop in MATLAB Simulink

The derivation starts from the inner loop. The block diagram of the inner loop can then be simplified as shown in Figure 4.7 and the simplified transfer function is denoted to be G_i .

$$F = (S - G_m F)(G_{IP,v} G_{C2}) \quad (4.50)$$

$$G_i = \frac{F}{S} = \frac{G_{IP,v} G_{C2}}{G_{IP,v} G_{C2} G_m + 1} \quad (4.51)$$

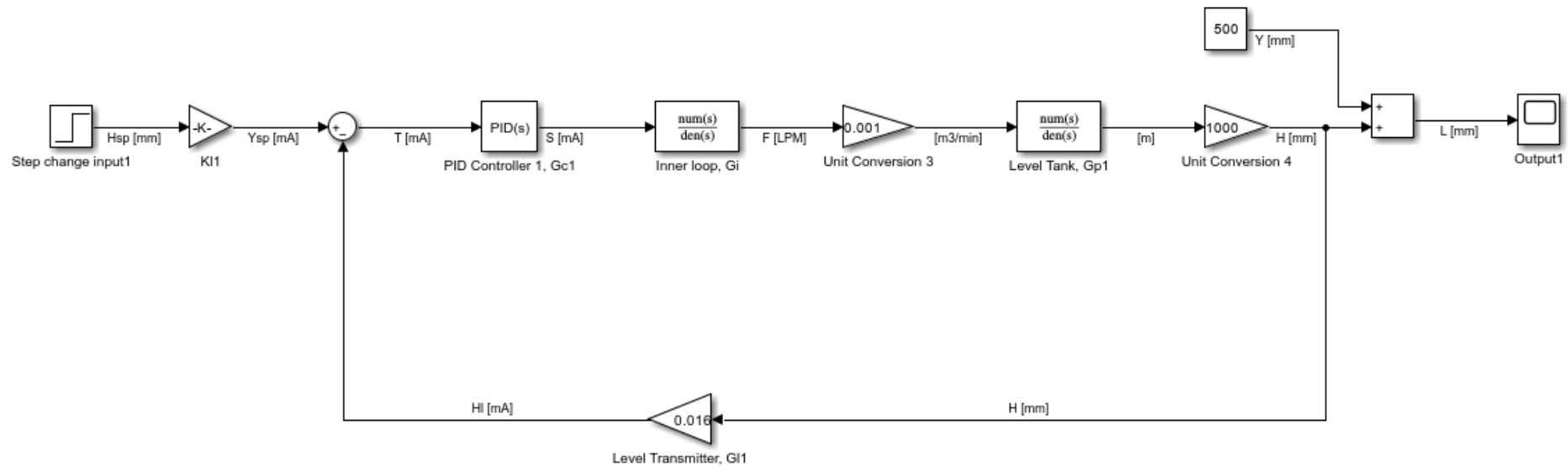


Figure 4.7: Simplified flow/level cascade control feedback loop in MATLAB Simulink

For the outer loop, the equation can be written and rearranged as follows:

$$(H_{sp}K_{l1} - G_{l1}H)G_{c2}G_iG_{p1} = H \quad (4.52)$$

$$\frac{H}{H_{sp}} = \frac{G_{c1}G_iG_{p1}K_{l1}}{G_{c1}G_iG_{p1}G_{l1} + 1} \quad (4.53)$$

Substitute equation (4.51) into equation (4.53), the following equations are obtained:

$$\frac{H}{H_{sp}} = \frac{G_{c1}G_{p1}K_{l1} \frac{G_{IP,v}G_{c2}}{G_{IP,v}G_{c2}G_m + 1}}{G_{c1}G_{p1}G_{l1} \frac{G_{IP,v}G_{c2}}{G_{IP,v}G_{c2}G_m + 1} + 1} \quad (4.54)$$

$$\frac{H}{H_{sp}} = \frac{G_{c1}G_{c2}G_{IP,v}G_{p1}K_{l1}}{G_{c1}G_{c2}G_{p1}G_{IP,v}G_{l1} + G_{c2}G_{IP,v}G_m + 1} \quad (4.55)$$

4.3 Value Assignment

After formulating the mathematical model, the next step is to simulate the developed model. However, before proceeding with the simulation, it is essential to assign values to all constants in the mathematical model to enable the required calculations. This section therefore provides a detailed explanation of how the values of all constants are determined, either through direct calculation, experimental measurement or by adopting values from relevant sources.

4.3.1 Level Tank

Under a steady state condition, it is reasonable to assume that the height of the liquid in the level tank, \bar{h} is given by 500 mm (the range of the height is 0 – 1000 mm). In addition, the valve coefficient C_v is equal to $0.5 \frac{LPM}{\sqrt{mm}}$ as given by the specification of the equipment. By substituting these values into equation (4.5),

$$0 = \bar{q}_i - 0.5\sqrt{500} \quad (4.56)$$

$$\bar{q}_i = 11.18 \text{ LPM} \quad (4.57)$$

Hence, the steady-state flowrate of the liquid circulating through the system is given by 11.18 LPM, which is a reasonable value as observed from experiments reported in Section 4.1. In addition, it is also desired to express all the quantities involved in the SI units, for the consistency in the calculation. From equation (4.56),

$$\bar{q}_i[\text{LPM}] = 0.5\sqrt{\bar{h}[\text{mm}]} \quad (4.58)$$

By multiplying equation (4.58) with appropriate factors, the C_v value in the unit of $\frac{m^3}{\text{min}\sqrt{m}}$ can be obtained, which is given by $0.01581 \frac{m^3}{\text{min}\sqrt{m}}$. The detailed calculation is shown below:

$$\bar{q}_i[\frac{m^3}{\text{min}}] = 0.0005\sqrt{\bar{h}[\text{mm}]} \quad (4.59)$$

$$\bar{q}_i[\frac{m^3}{\text{min}}] = 0.0005\sqrt{1000\bar{h}[\text{m}]} \quad (4.60)$$

$$C_v = 0.0005\sqrt{1000} = 0.01581 \frac{m^3}{\text{min}\sqrt{m}} \quad (4.61)$$

Additionally, the radius of the level tank is measured as 0.08 m from the actual equipment, hence the cross-sectional area of the tank is calculated as:

$$A = \pi r^2 = 0.02 \text{ m}^2 \quad (4.62)$$

Substituting values of \bar{h} , C_v and A into equation (4.16), the transfer function of change of the height of liquid in the level tank process is given by:

$$G_p = \frac{H'(s)}{Q_i'(s)} = \frac{\frac{2\sqrt{0.5}}{0.01581}}{[\frac{2\sqrt{0.5}}{0.01581}0.02s+1]} \quad (4.63)$$

4.3.2 I/P Transducer and Control Valve

To simulate the mathematical model developed in Section 4.2, it is necessary to include the dynamic behavior of the I/P transducer and control valve. Figure 4.8 illustrates the signal flow involving these instruments within the control system. The controller sends an electric signal (in mA) to the I/P transducer, which converts it into a pneumatic signal (in psi). This pneumatic signal adjusts the valve opening, thereby regulating the flow rate (in LPM). The combined dynamics of the I/P transducer and valve can be represented by the following transfer function:

$$K_{IP} \left(\frac{K_v}{\tau_v s + 1} \right) = \frac{K_{IP} K_v}{\tau_v s + 1} \quad (4.64)$$

To perform the simulation, the parameters K_{IP} , K_v and τ_v must be determined. However, specific data for the gain and time constant of these instruments is unavailable, as they are permanently installed on the equipment and cannot be removed for detailed characterization. This presents a challenge in directly measuring the model parameters.

Fortunately, since the I/P transducer and control valve are typically used together as a fixed pair (as shown in Figure 4.8), it is not necessary to determine K_{IP} and K_v individually. Instead, only the product $K_{IP} K_v$ needs to be estimated, along with the valve time constant, τ_v . These values are estimated by comparing the experimental response of the system with the simulation results. The unknown parameters are then iteratively tuned until the simulated behavior closely matches the observed system response.

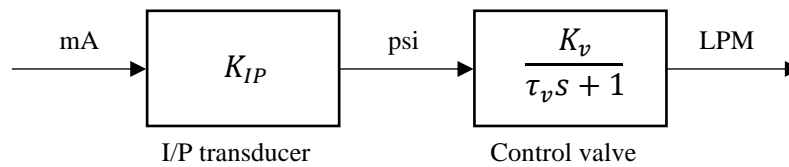


Figure 4.8: Block diagram with transfer function of I/P transducer and control valve

Figures 4.9 and 4.10 illustrate the simulated and experimental responses of the flow rate to a setpoint change (from 10 LPM to 15 LPM) for different proportional band (PB) values. The responses are shown at two different process gains: $K_{IP}K_v = 0.5 \frac{\text{LPM}}{\text{mA}}$ (Figure 4.9) and $K_{IP}K_v = 1 \frac{\text{LPM}}{\text{mA}}$ (Figure 4.10), with a constant process time delay $\tau_v = 2.3$ for both figures. It is observed that while both sets of responses exhibit an offset, the configuration with $K_{IP}K_v = 1 \frac{\text{LPM}}{\text{mA}}$ produces a closer match between the simulation and experimental results across the different PB values.

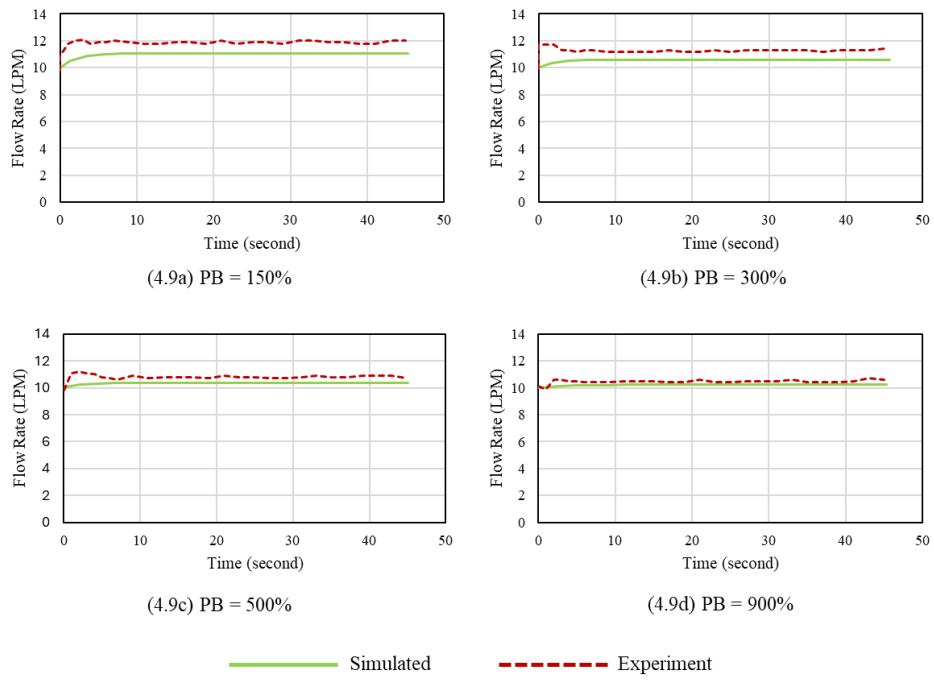


Figure 4.9: Response of simulated and experimental flow rate (controlled variable) toward the set point change (from 10 LPM to 15 LPM) at $K_{IP}K_v = 0.5 \frac{\text{LPM}}{\text{mA}}$ and $\tau_v = 2.3$ regulated by proportional controller

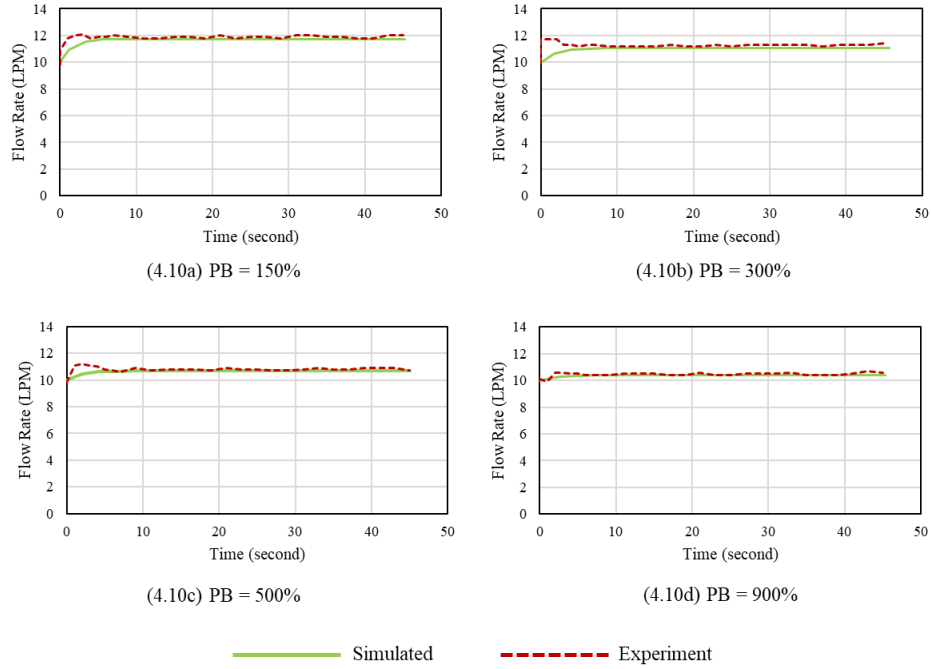


Figure 4.10: Response of simulated and experimental flow rate (controlled variable) toward the set point change (from 10 LPM to 15 LPM) at $K_{IP}K_v = 1 \frac{\text{LPM}}{\text{mA}}$ and $\tau_v = 2.3$ regulated by proportional controller

Figures 4.11 and 4.12 demonstrate the effect of varying the integral action on the flow rate response while maintaining a constant PB value at 150%. From Figure 4.11, it is evident that introducing integral action improves the steady-state accuracy and reduces offset, with relatively good agreement between the simulated and experimental results, particularly for moderate values of the integral gain.

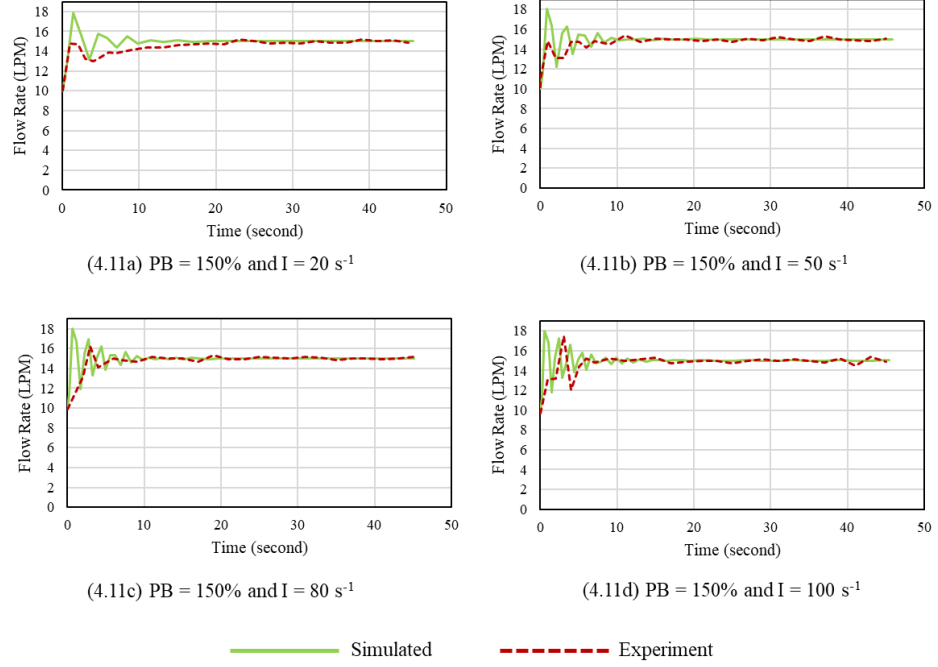


Figure 4.11: Response of simulated and experimental flow rate (controlled variable) toward the set point change (from 10 LPM to 15 LPM) at $K_{IP}K_v = 0.5 \frac{\text{LPM}}{\text{mA}}$ and $\tau_v = 2.3$ regulated by proportional and integral controller

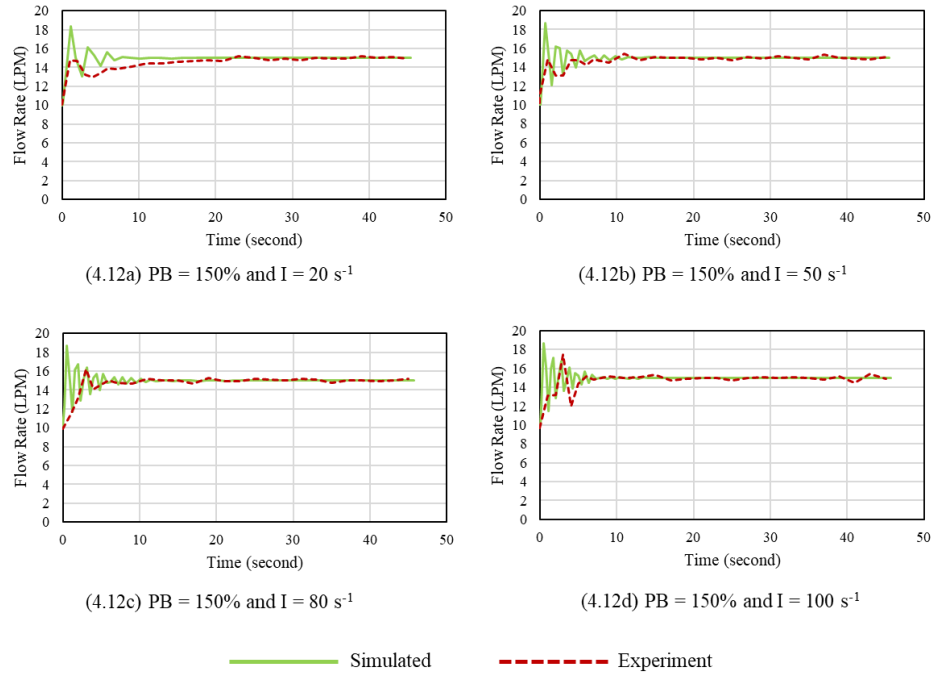


Figure 4.12: Response of simulated and experimental flow rate (controlled variable) toward the set point change (from 10 LPM to 15 LPM) at $K_{IP}K_v = 1 \frac{\text{LPM}}{\text{mA}}$ and $\tau_v = 2.3$ regulated by proportional and integral controller

Although Figure 4.11 indicates better similarity between the simulation and experimental results when compared to Figure 4.12, the comparison between Figures 4.9 and 4.10 reveals that the higher process gain at $K_{IP}K_v = 1 \frac{\text{LPM}}{\text{mA}}$ yields a more accurate match. Therefore, it is inferred that $K_{IP}K_v = 1 \frac{\text{LPM}}{\text{mA}}$ is a more suitable process gain for this system under the tested conditions.

Figures 4.13, 4.14, and 4.15 depict the simulated and experimental responses of the flow rate to a set point change (from 10 LPM to 15 LPM) for different proportional band (PB) values. The responses are evaluated at three time constants for control valve: $\tau_v = 0.2$ (Figure 4.13), $\tau_v = 1.5$ (Figure 4.14), and $\tau_v = 2.3$ (Figure 4.15) with a constant process gain $K_{IP}K_v = 1 \frac{\text{LPM}}{\text{mA}}$ for all three figures. Among these, $\tau_v = 0.2$ demonstrates the closest agreement between the simulated and experimental results.

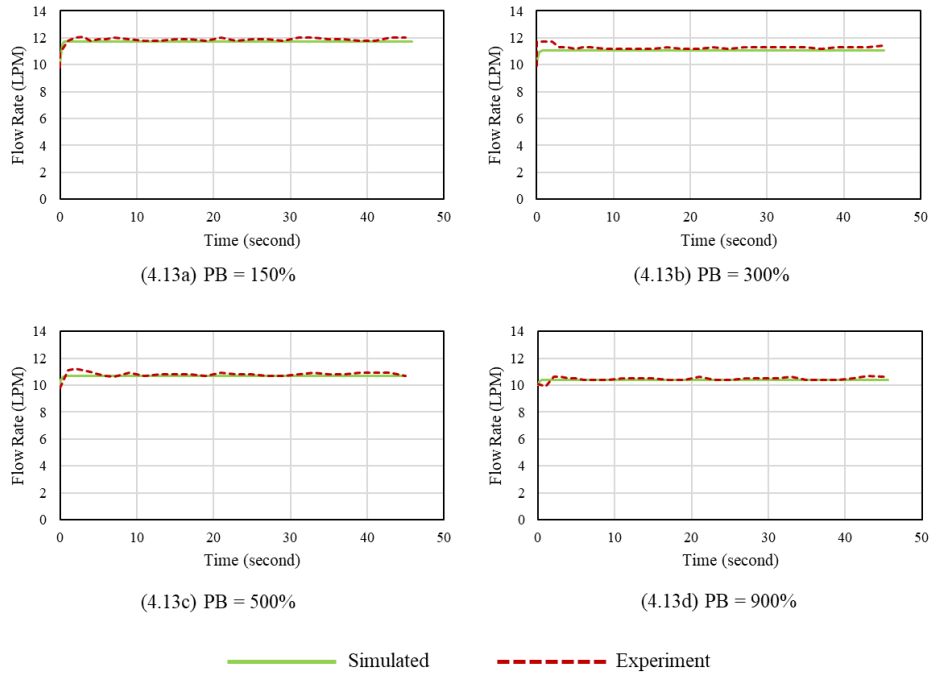


Figure 4.13: Response of simulated and experimental flow rate (controlled variable) toward the set point change (from 10 LPM to 15 LPM) at $K_{IP}K_v = 1 \frac{\text{LPM}}{\text{mA}}$ and $\tau_v = 0.2$ regulated by proportional controller

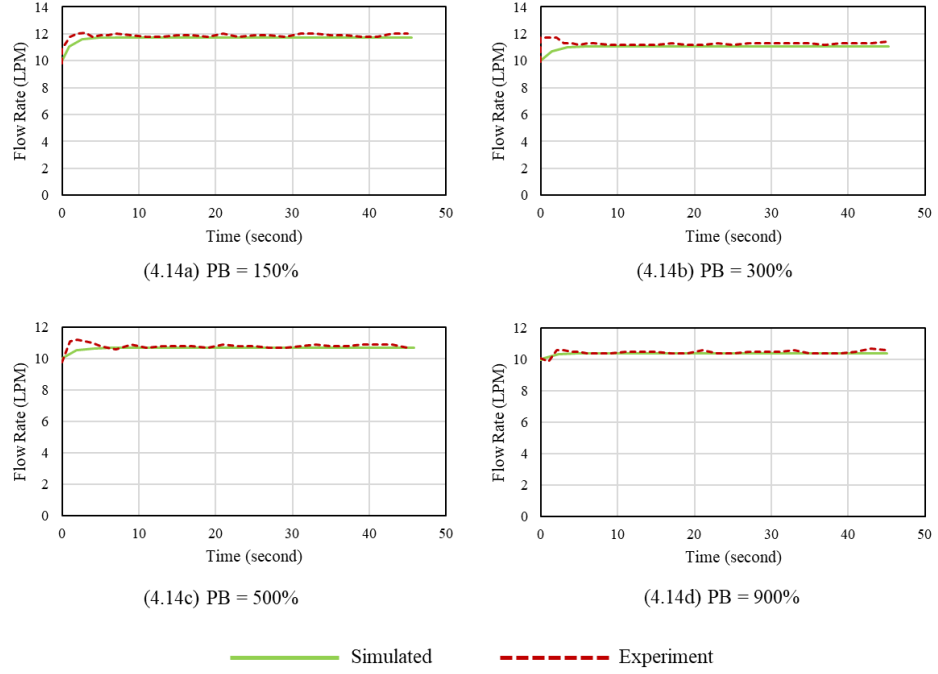


Figure 4.14: Response of simulated and experimental flow rate (controlled variable) toward the set point change (from 10 LPM to 15 LPM) at $K_{IP}K_v = 1 \frac{LPM}{mA}$ and $\tau_v = 1.5$ regulated by proportional controller

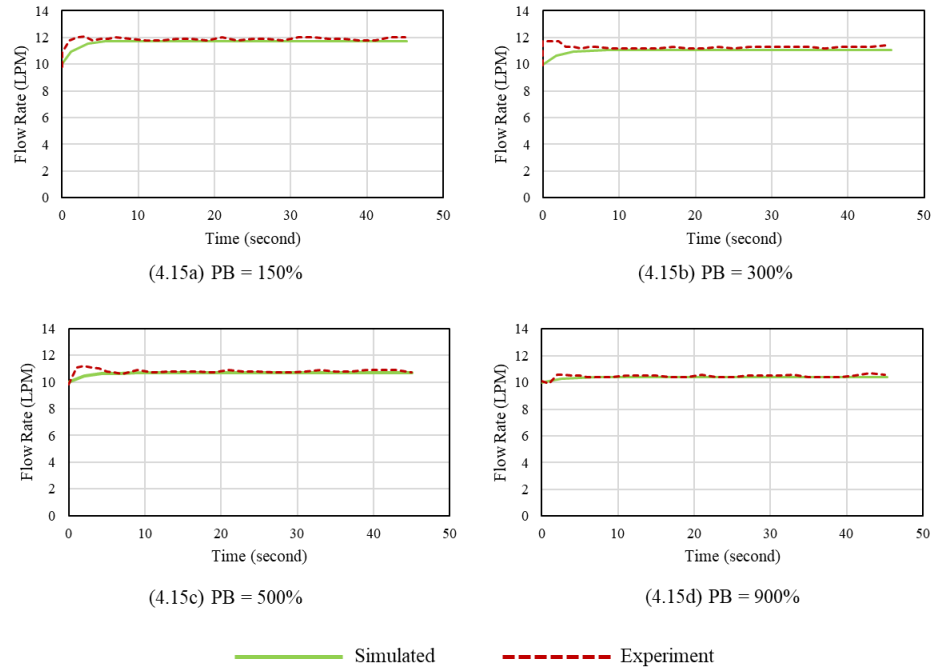


Figure 4.15: Response of simulated and experimental flow rate (controlled variable) toward the set point change (from 10 LPM to 15 LPM) at $K_{IP}K_v = 1 \frac{LPM}{mA}$ and $\tau_v = 2.3$ regulated by proportional controller

Figures 4.16, 4.17, and 4.18 illustrate the simulated and experimental responses of the flow rate to the same set point change, but with the addition of an integral controller. These responses are analyzed for different integral gain (I) values while maintaining a constant PB value of 150% ($P = 0.67$). The time constants examined are $\tau_v = 0.2$ (Figure 4.16), $\tau_v = 1.5$ (Figure 4.17), and $\tau_v = 2.3$ (Figure 4.18) with a constant process gain $K_{IP}K_v = 1 \frac{LPM}{mA}$ for all three figures. In this case, $\tau_v = 2.3$ emerges as the most suitable value.

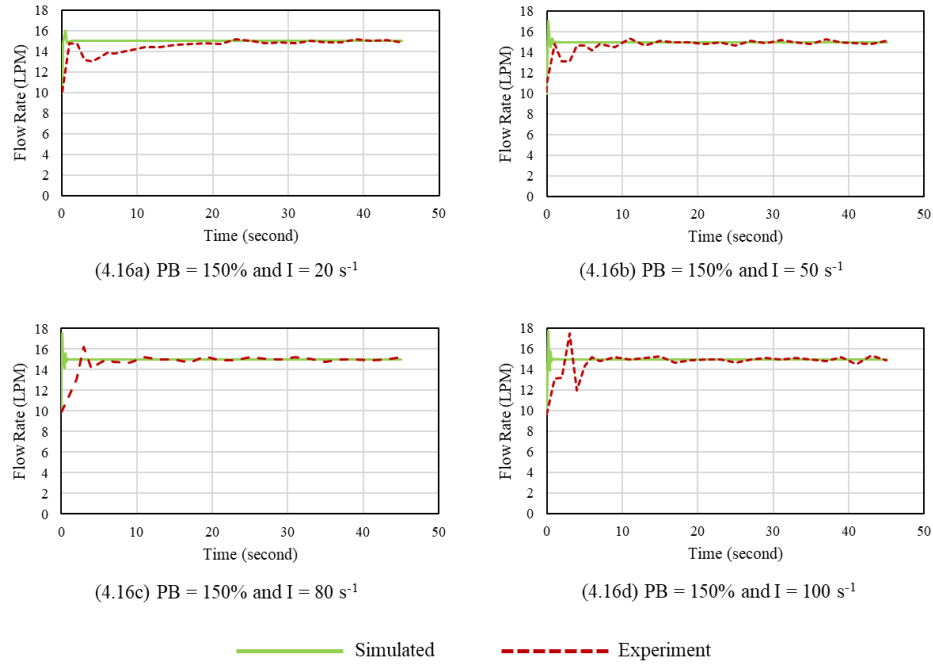


Figure 4.16: Response of simulated and experimental flow rate (controlled variable) toward the set point change (from 10 LPM to 15 LPM) at $K_{IP}K_v = 1 \frac{LPM}{mA}$ and $\tau_v = 0.2$ regulated by proportional and integral controller

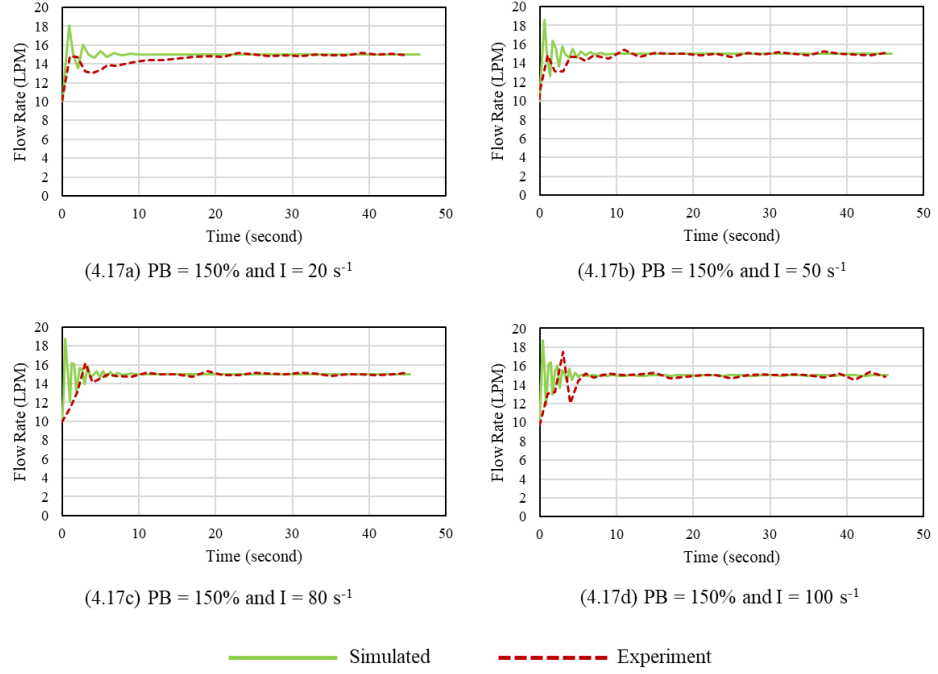


Figure 4.17: Response of simulated and experimental flow rate (controlled variable) toward the set point change (from 10 LPM to 15 LPM) at $K_{IP}K_v = 1 \frac{\text{LPM}}{\text{mA}}$ and $\tau_v = 1.5$ regulated by proportional and integral controller

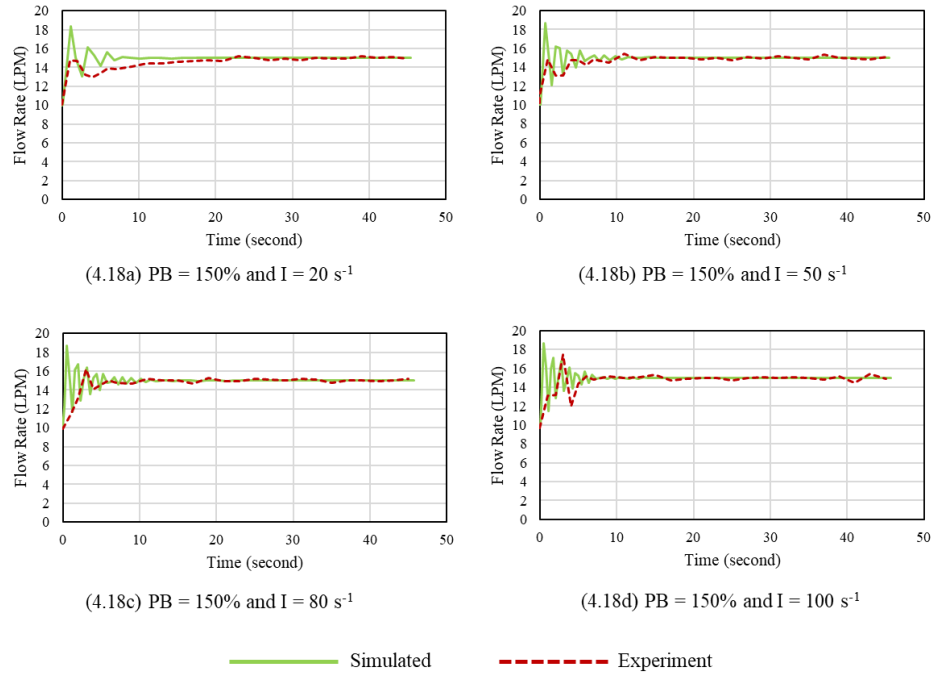


Figure 4.18: Response of simulated and experimental flow rate (controlled variable) toward the set point change (from 10 LPM to 15 LPM) at $K_{IP}K_v = 1 \frac{\text{LPM}}{\text{mA}}$ and $\tau_v = 2.3$ regulated by proportional and integral controller

While $\tau_v = 0.2$ is optimal for the proportional controller alone, it causes the system to respond too aggressively when the integral controller is introduced, leading to significant discrepancies between the simulated and experimental results. In contrast, $\tau_v = 2.3$ provides a balanced performance where it aligns well with the experimental stabilization time when the integral controller is used and does not compromise performance excessively when only the proportional controller is active.

After adjusting the multiplied gain of $K_{IP}K_v$ and the time constant of the control valve τ_v , the parameters are set where the simulated response of the output flow rate resembles the experimental response output flow rate. The combined transfer function of the I/P transducer and the control valve, $G_{v,IP}$ is shown in equation (4.67).

$$K_{IP}K_v = 1 \frac{LPM}{mA} \quad (4.65)$$

$$\tau_v = 2.3 \quad (4.66)$$

$$G_{IP,v} = \frac{1}{2.3s+1} \quad (4.67)$$

4.3.3 Transmitter

Based on information available from the manual of the control system, the gain of the flow transmitter, K_m and level transmitter, K_l are calculated as follows:

$$K_m = \frac{(20-4) mA}{(20-0) LPM} = 0.8 \frac{mA}{LPM} \quad (4.67)$$

$$K_l = \frac{(20-4) mA}{(1000-0) mm} = 0.016 \frac{mA}{mm} \quad (4.68)$$

4.4 Simulation Results

After determining all the parameters of each instrument and the level process, simulations were conducted using MATLAB Simulink. This section presents a

comparison between the simulated and experimental output flow rates for the flow control system. As the level control and flow/level cascade control experiments were not conducted, only simulation results for these control systems are provided without experimental comparison. Nevertheless, the trends and behavior observed in each simulation will be analyzed and discussed.

4.4.1 Flow Control

A step change of 5 LPM is applied to all flow control simulations for 45 s and their outputs are compared and analysed.

Figure 4.19 presents a comparison of different proportional (P) controller values when the integral (I) and derivative (D) controllers are not utilised. The results indicate that a higher P value reduces the steady-state error (offset from the set point once it achieves steady-state) and a faster response, while lower P values result in larger offsets and slower response. However, using only a P controller will still result in an offset; the difference lies in whether the offset is larger or smaller.

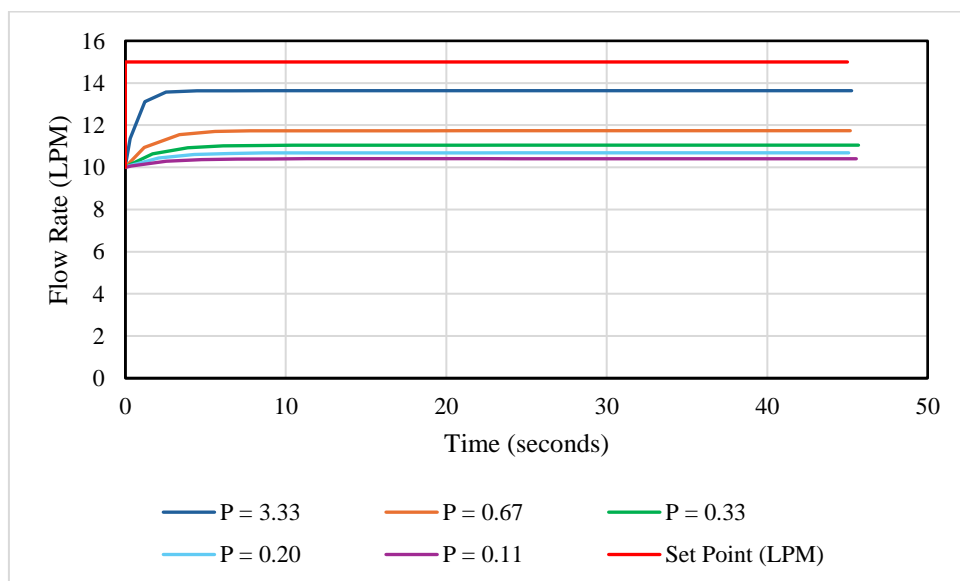


Figure 4.19: Response of simulated flow rate (controlled variable) toward the set point change (from 10 LPM to 15 LPM) regulated by proportional controller with different P values

Figure 4.20 presents a comparison between the simulated and experimental results for $P = 0.67$, 0.33 and 0.11 . The simulated results show a high degree of similarity to the experimental data, particularly in the offset of the steady-state flow rate from the set point. However, some discrepancies are observed during the transient phase at the beginning of the graph for all three comparisons. These differences may be attributed to the overly idealized nature of the simulation model. Despite this, both the simulated and experimental results consistently demonstrate that using a proportional (P) controller alone leads to a steady-state error, resulting in a persistent offset between the output flow rate and the set point.

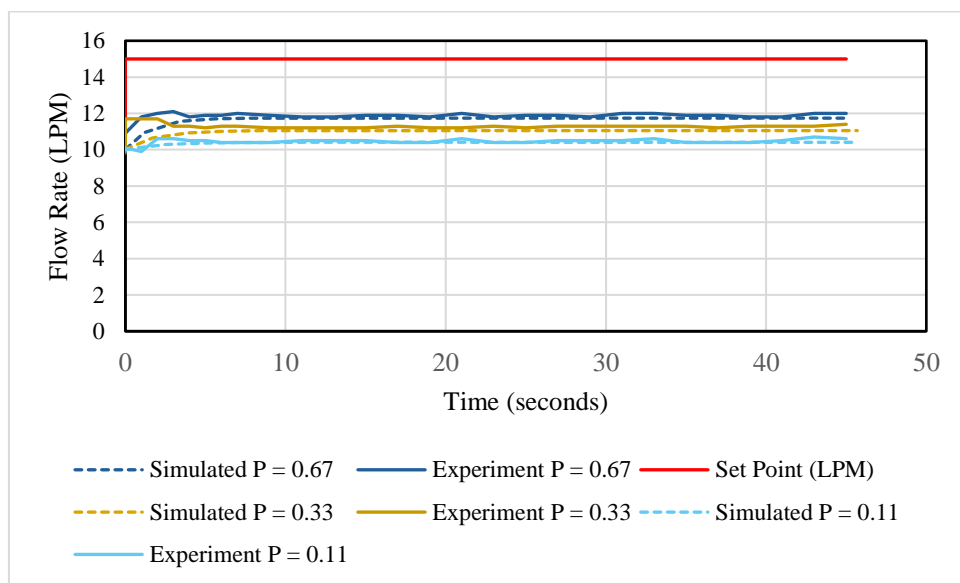


Figure 4.20: Comparison of simulated and experimental flow rate (controlled variable) toward the set point change (from 10 LPM to 15 LPM) regulated by proportional controller with different P values

Figure 4.21 and 4.22 illustrates the influence of the integral controller when the proportional controller is fixed at $P = 0.67$. A larger integral gain introduces a larger overshoot when a step change is applied, as the system reacts more aggressively to eliminate error. Conversely, a smaller integral gain gradually eliminates the steady-state error introduced by the proportional controller. This demonstrates the integral controller's role in eliminating long-term errors while maintaining system stability. This trend is consistent with the experiment findings as shown in Figure 4.2.

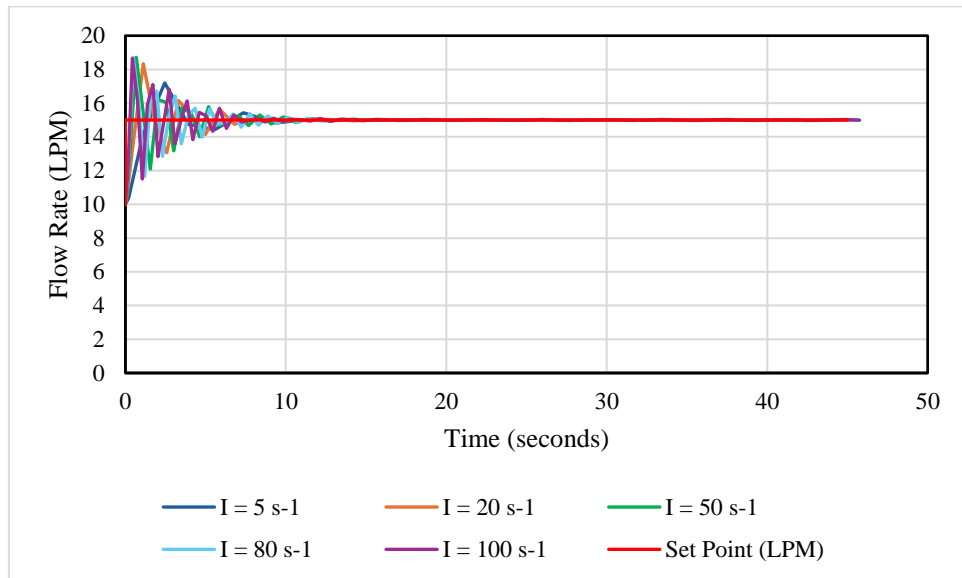


Figure 4.21: Response of simulated flow rate (controlled variable) toward the set point change (from 10 LPM to 15 LPM) regulated by proportional and integral controller with different I values and constant $P = 0.67$

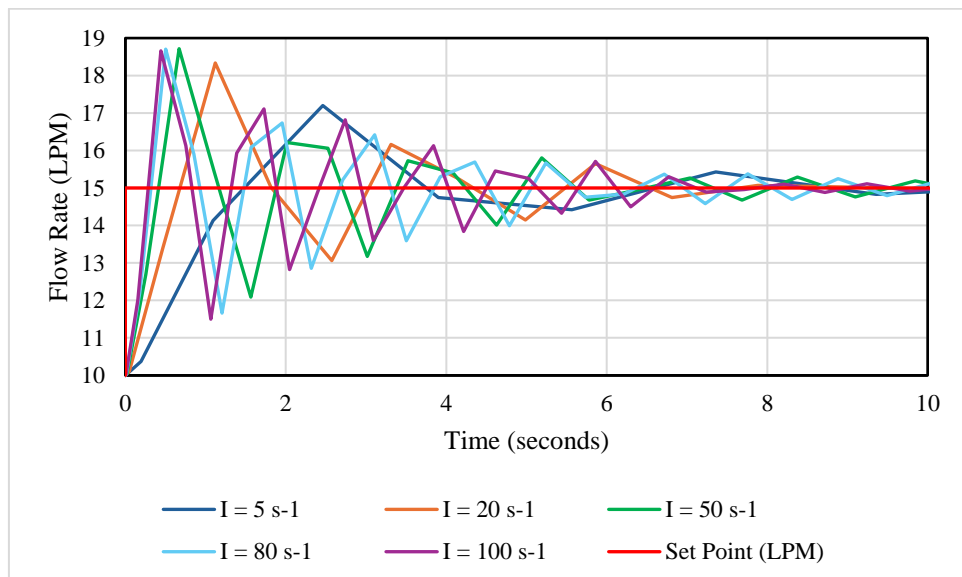


Figure 4.22: Detailed view of early-stage system response in Figure 4.21

Figure 4.23 depicts the comparison between the simulated and experimental results for constant $P = 0.67$, varying $I = 20 \text{ s}^{-1}$ and 100 s^{-1} . From both the experimental and simulated results in both scenarios, the controlled flow rate ultimately achieve the set point of 15 LPM. However, during the initial phase of the response, noticeable discrepancies can be observed between the two graphs. The simulated results exhibit a more aggressive reaction compared to the experimental data, leading to increased

oscillations before gradually stabilizing. Additionally, the simulated response demonstrates a significantly larger overshoot than the experimental results. These differences may be attributed to various assumptions made during the modelling process, particularly regarding the gain settings of the control valve and transducer, as well as the time constant of the control valve. In real life, the dynamic behaviour of these components may differ from the idealised values used in the simulation, leading to the non-uniformity in the initial system response.

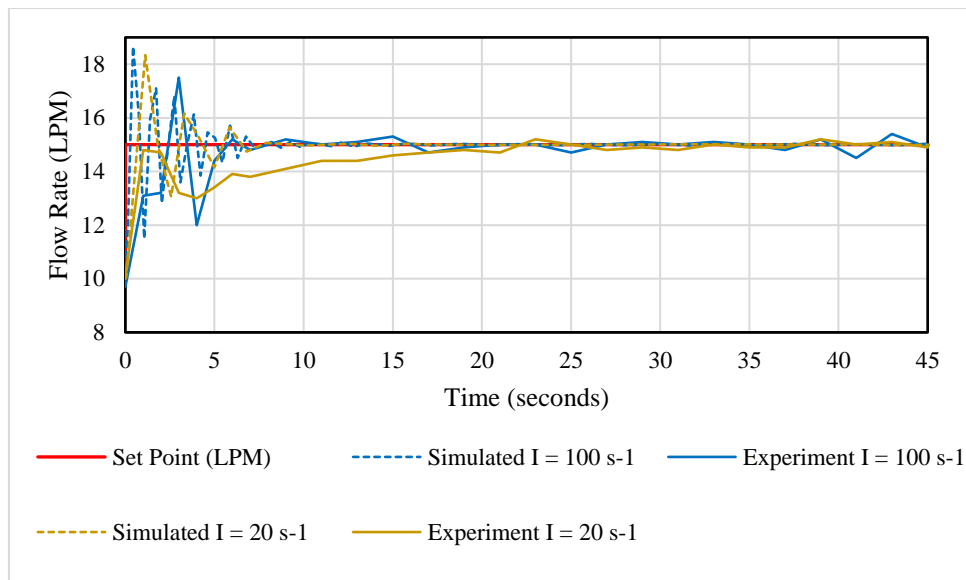


Figure 4.23: Comparison of simulated and experimental flow rate (controlled variable) toward the set point change (from 10 LPM to 15 LPM) regulated by proportional and integral controller with different I values and constant $P = 0.67$

Figure 4.24 analyzes the effect of varying the derivative time (D) in the PID controller while keeping the proportional gain ($P = 2/3$), integral time ($I = 20 \text{ s}^{-1}$), and filter coefficient ($N = 3$) constant. The results in Figure 4.25 indicate that the derivative component plays a significant role in reducing the overshoot typically introduced by the integral action. At lower D values, such as 2 s and 3 s, the system exhibits a higher overshoot and increased oscillations. As the value of D increases, the response becomes progressively more damped, leading to a noticeable reduction in overshoot and improved system stability. The trend is indeed consistent with the experimental results as shown in Figure 4.3.

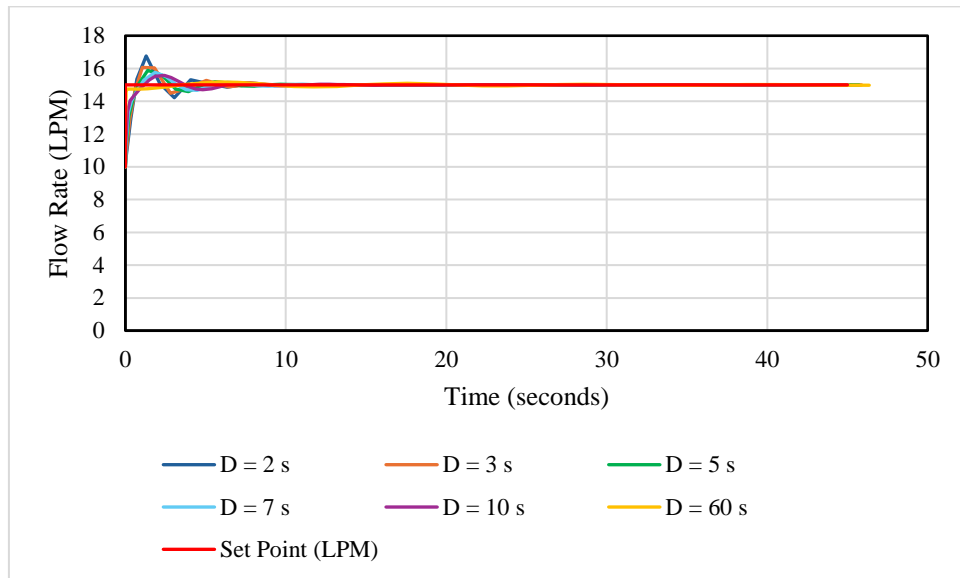


Figure 4.24: Response of simulated flow rate (controlled variable) toward the set point change (from 10 LPM to 15 LPM) regulated by proportional, integral, and derivative controller with different D values and constant $P = 0.67$, $I = 20 \text{ s}^{-1}$ and $N = 3$

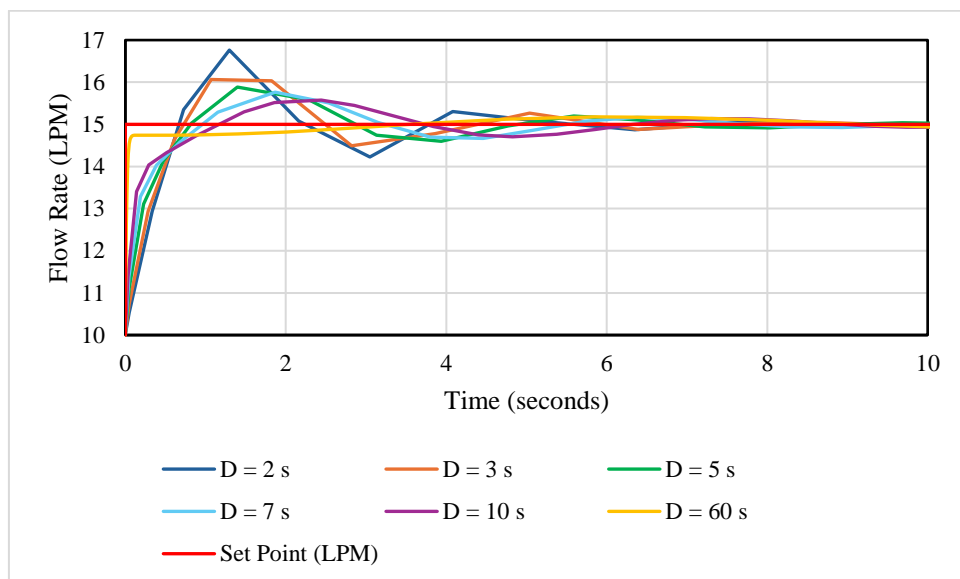


Figure 4.25: Detailed view of early-stage system response in Figure 4.24

Figure 4.26 presents a comparison between the simulated and experimental flow rate responses for the controller parameters $P = 0.67$, $I = 20 \text{ s}^{-1}$ and $N = 3$ while varying $D = 3 \text{ s}$, 5 s , and 7 s . Both the simulated and experimental response ultimately reach the set point of 15 LPM, with visible oscillations during the transient phase. However, the simulated response reacts more rapidly and exhibits a slight overshoot compared to the experimental response, which shows in a slower but more damped

behavior. When compared to Figure 4.23 where only the PI controller is utilised, it is evident that the inclusion of the derivative component helps to smoothen the system response, significantly reducing both overshoot and oscillations. This highlights the effectiveness of the derivative controller in improving system stability and transient performance.

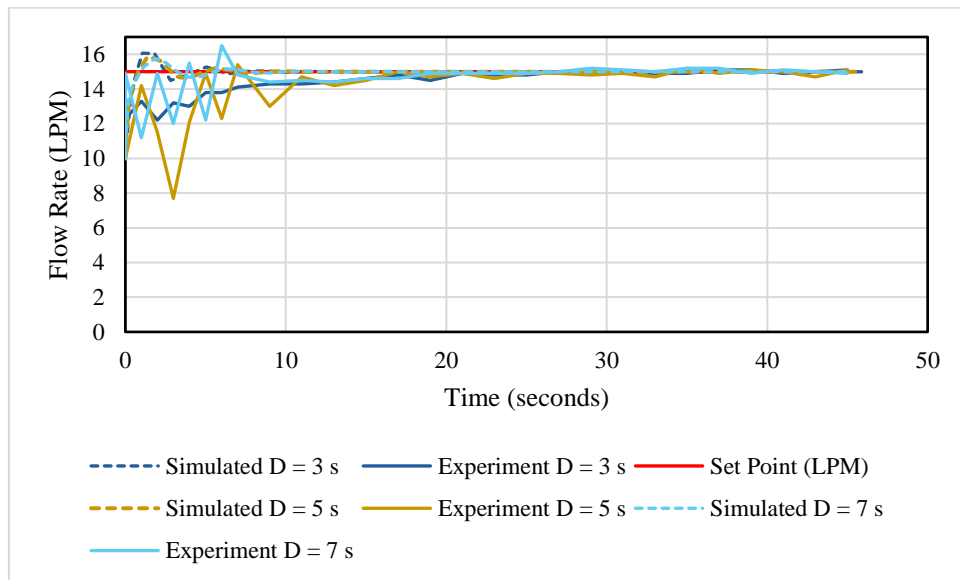


Figure 4.26: Comparison of simulated and experimental flow rate (controlled variable) toward the set point change (from 10 LPM to 15 LPM) regulated by proportional, integral and derivative controller with different D values and constant $P = 0.67$, $I = 20 \text{ s}^{-1}$, and $N = 3$

These findings highlight the individual roles of P, I, and D controllers and their combined effects on system performance. While the proportional controller primarily reduces the offset, the integral controller eliminates steady-state error, and the derivative controller can help to reduce overshoot while stabilize the response.

4.4.2 Level Control

In this subsection, the simulation results of the level control system's response to a step change in the setpoint are presented. Similar to the previous subsection, the effects of the P, I, and D values on the controlled variable (liquid level in the tank) are thoroughly

analyzed. A step change of 250 mm (from 500 mm to 750 mm) is applied in all simulations, and the system response over the first 200 seconds is recorded, compared, and discussed.

Figure 4.27 compares the performance of a proportional (P) controller at various gain settings in a level control system, operating without integral (I) or derivative (D) components. At a low gain of $P = 0.1$, the system exhibits a very slow response, with minimal change in output height. Under this scenario, the steady-state value is still very far away from the set point, giving a very high offset. Increasing the gain to $P = 0.5$ and $P = 1$ enhances the response speed, but a significant steady-state error remains. When the gain is further increased to $P = 3$, the system responds much more rapidly to the step change and the offset during the steady state has been significantly reduced. However, a slight overshoot is observed due to the aggressive nature of the higher proportional gain. Despite improvements in response time, all cases exhibit a persistent steady-state offset, which is a known limitation of using a P controller alone. The magnitude of this error varies with the gain setting, but it cannot be completely eliminated without incorporating integral action into the control strategy after a set point change.

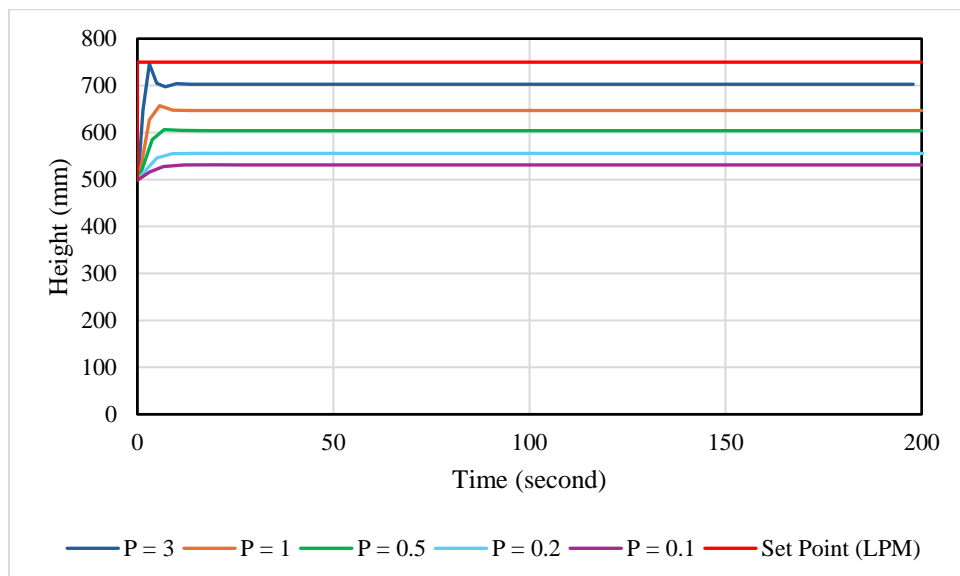


Figure 4.27: Response of simulated liquid level (controlled variable) toward the set point change (from 10 LPM to 15 LPM) regulated by proportional controller at different P values

Figure 4.28 compares the performance of an integral (I) controller at varying gain settings in a level control system, where the proportional gain is fixed at $P = 1$ without derivative (D) control. Figure 4.29 illustrates that at $I = 0.1 \text{ s}^{-1}$, the system exhibits a slow response, requiring the longest time to reach both steady state and the set point of 750 mm. Increasing the integral gain to $I = 0.2 \text{ s}^{-1}$ significantly improves the response speed, achieving a balanced performance, reaching steady state and the set point within approximately 30 seconds without overshoot. However, further increasing the integral gain to $I = 0.5 \text{ s}^{-1}$, and 1 s^{-1} produces more aggressive responses towards the step change. These higher gains introduce undesirable overshoot and oscillations around the set point which is a consequence of excessive integral action. When the integral gain is increased to 2 s^{-1} , the system is unable to stabilize and oscillations increase in amplitude as time passes. While higher integral gains solve offset errors, they can also destabilize the system by oscillatory behavior and introduce overshoot.

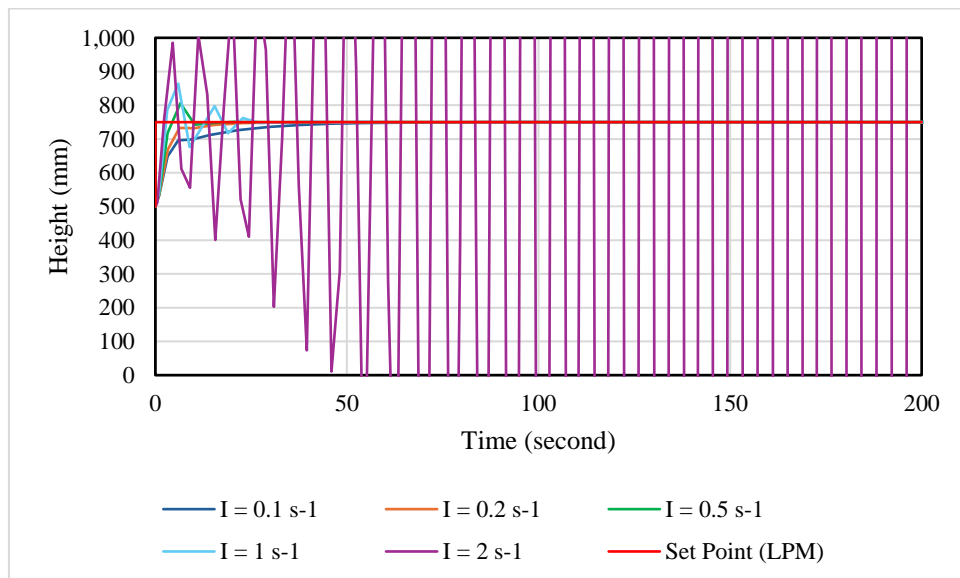


Figure 4.28: Response of simulated liquid level (controlled variable) toward the set point change (from 10 LPM to 15 LPM) regulated by proportional and integral controller with different I values and constant $P = 1$

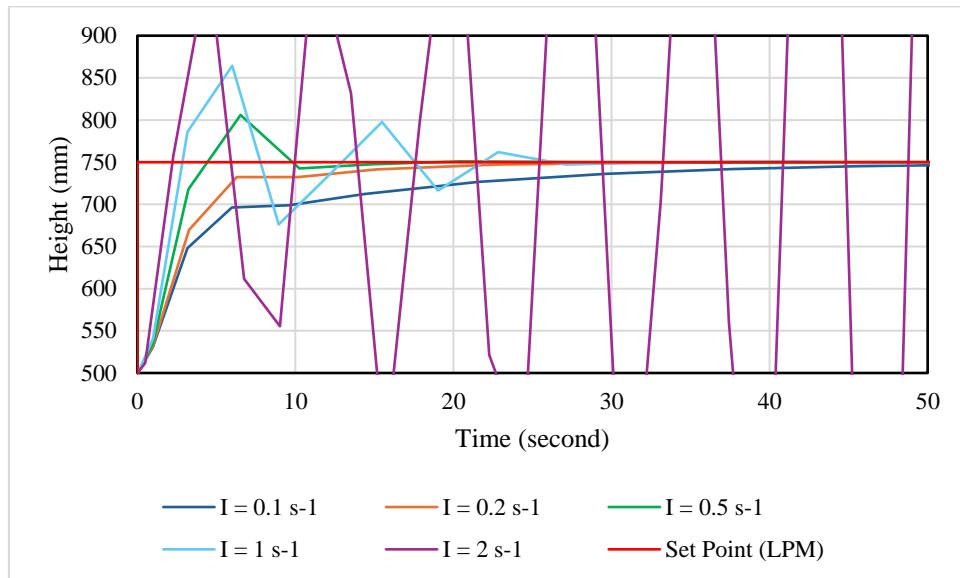


Figure 4.29: Detailed view of early-stage system response in Figure 4.28

Figure 4.30 illustrates the effect of varying the derivative (D) parameter on system performance, with the proportional gain set to $P = 1$, integral gain to $I = 0.2 \text{ s}^{-1}$, and derivative filter coefficient to $N = 3$. Figure 4.31 shows that a properly tuned derivative action effectively reduces overshoot and improves damping. However, when the derivative time becomes too large ($D = 20 \text{ s}$), the system exhibits prolonged oscillations before settling, though the amplitude of these oscillations is significantly smaller compared to Figure 4.28, where no derivative action is applied. When tuned correctly, the derivative minimizes overshoot and stabilizes the response. However, if the derivative action is too strong, it can slow convergence and introduce persistent but mild oscillations, as seen at higher D values.

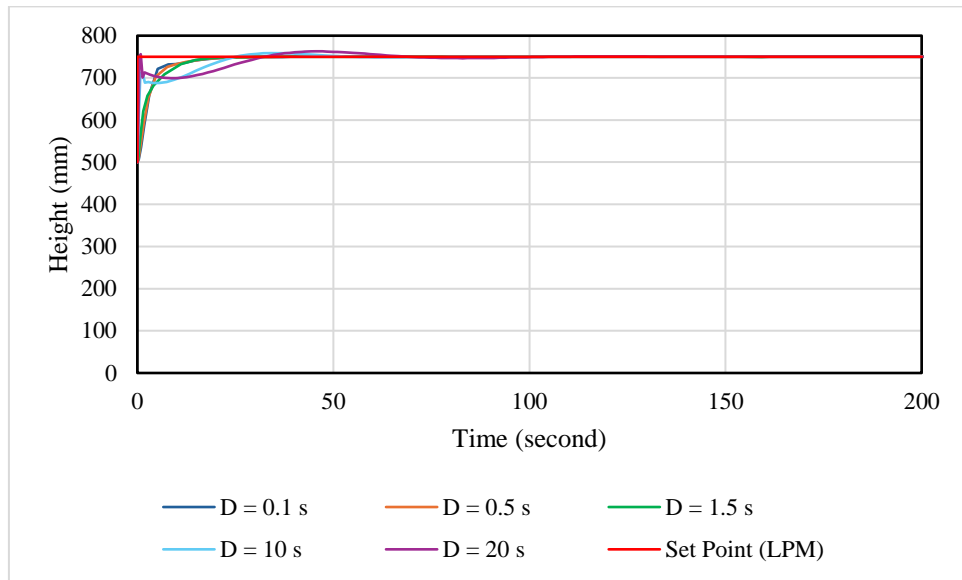


Figure 4.30: Response of simulated liquid level (controlled variable) toward the set point change (from 10 LPM to 15 LPM) regulated by proportional, integral, and derivative controller with different D values and constant $P = 1$, $I = 0.2 \text{ s}^{-1}$ and $N = 3$

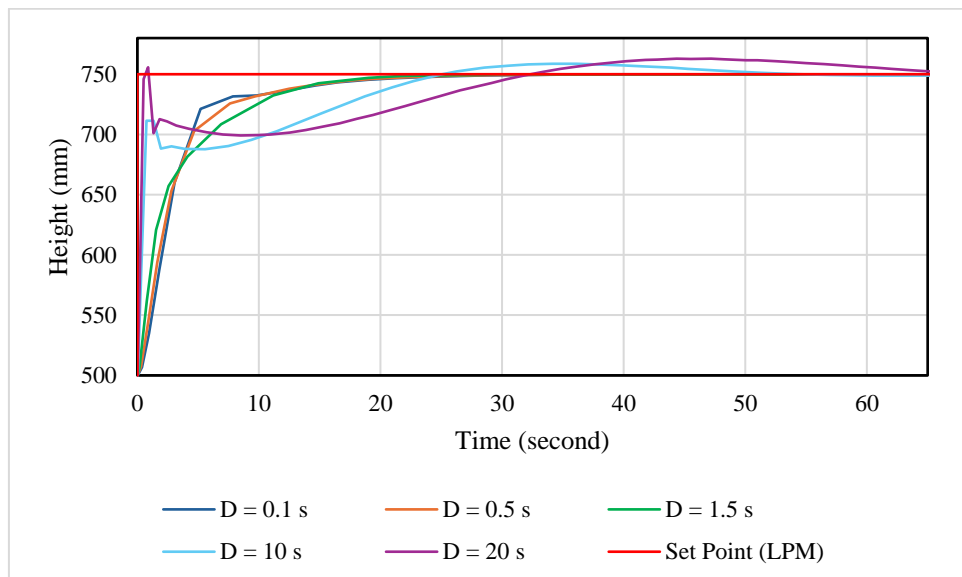


Figure 4.31: Detailed view of early-stage system response in Figure 4.30

These findings emphasize the distinct functions of the P, I, and D controllers, as well as their combined influence on system performance. The proportional controller focuses on minimizing the offset, the integral controller addresses and eliminates steady-state error, and the derivative controller minimizes overshoot and stabilizes the response. The behavior observed in all three simulation types for the level control system aligns with the findings reported by Seborg et al. (2016). An increase in

proportional gain leads to a faster system response but introduces oscillations before eventually stabilizing with an offset. Increasing the integral gain (i.e., decreasing the integral time) results in a slower return of the controlled variable to the setpoint, but it effectively eliminates the offset. Conversely, a large derivative time tends to amplify noise and induce oscillations, whereas a smaller derivative time can enhance the system response by reducing response time, oscillations, and deviation (Seborg et al., 2016).

4.4.3 Flow/Level Cascade Control

In this subsection, the simulation results of the cascade control system's response to a step change in the set point are presented. As with the previous cases, the impact of tuning parameters, specifically the P, I, and D values of both the level (primary) controller on the system performance is analyzed in detail. A 250 mm step change (from 500 mm to 750 mm) is introduced to the setpoint of the primary controller, and the response of the controlled variable (liquid level) is observed over a 200-second period. The results are compared to evaluate the effectiveness of the cascade structure in improving control performance relative to single-loop configurations.

In this system, cascade control consists of an outer loop and an inner loop, working together to improve system stability and performance. The level (primary) controller is denoted as G_{c1} while the flow (secondary) controller is denoted as G_{c2} , while their controller settings are denoted as P_1, I_1, D_1 , and P_2, I_2, D_2 respectively. The values of G_{c2} are kept constant at $P_2 = 0.67, I_2 = 20 \text{ s}, D_2 = 3$. The derivative filter coefficient N is kept constant at 3 for both controllers (as long as the derivative controller is applied). The settings of the level (primary) controller is varied to examine the effect of the controller settings on response of the controlled variable toward the set point change.

Figure 4.32 illustrates the response of the tank level (height) over time under varying proportional gain (P_1) settings in the primary level controller, G_{c1} . As seen in the graph, increasing the proportional gain (P_1) reduces the steady-state error, bringing

the output closer to the set point. However, higher values of P_1 , can induce more oscillations and reduce system stability. This causes the output to overshoot a little and oscillate around the set point for a longer period before gradually settling. On the other hand, a very low P_1 value, such as 0.1, results in a sluggish response with a large steady-state error. Although the system remains stable, it fails to reach the set point and stabilizes below it. Among the tested values, $P_1 = 1$ offers the most favorable compromise between responsiveness and stability. The system reaches a relatively smooth response with minimal oscillations and achieves a final height approximately 90 mm below the desired set point. While some offset remains, this controller setting avoids excessive overshoot and maintains better overall control performance compared to higher P_1 values.

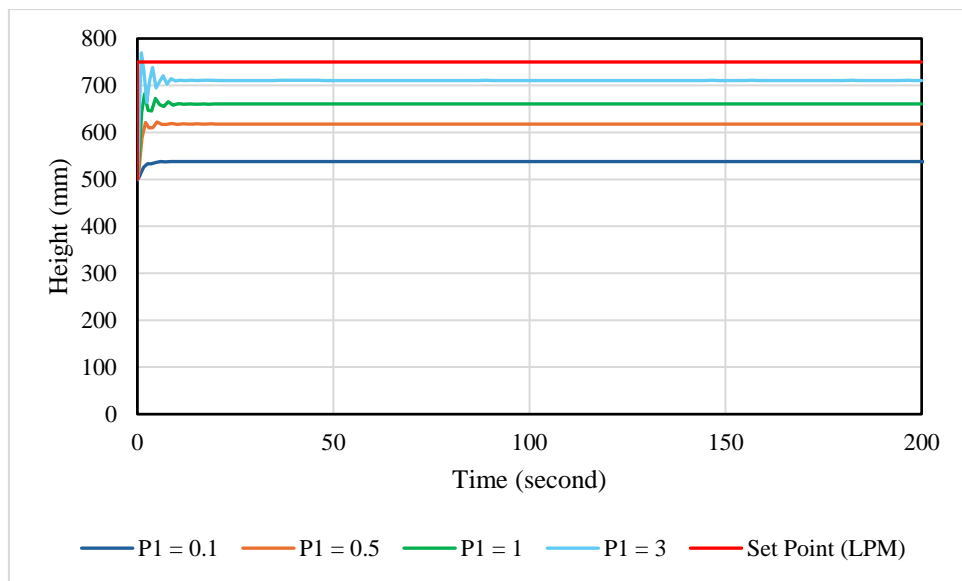


Figure 4.32: Response of simulated liquid level (controlled variable) toward the set point change (from 10 LPM to 15 LPM) regulated by proportional controller with different P_I values

Figure 4.33 presents the tank level response over time for various integral gain I_1 settings in the level controller G_{c1} . As shown in Figure 4.34 with the proportional gain fixed at $P_I = 1$ and the integral gain set to $I_1 = 0.2 \text{ s}^{-1}$, the system exhibits slight oscillations without any overshoot. It stabilizes at the set point of 750 mm in approximately 25 seconds, showing good balance between response speed and stability. This setting effectively eliminates the steady-state error introduced by the proportional

controller alone, without significantly compromising system performance. As the integral gain increases to $I_1 = 0.5 \text{ s}^{-1}$, and 1 s^{-1} , the system begins to display increasingly larger oscillations and larger overshoots. The damping decreases, and the time taken to stabilize becomes longer. These oscillations demonstrate that a higher integral action can lead to excessive correction and instability if not properly tuned. Further increasing I_1 to 2.5 s^{-1} , the system becomes unstable. The oscillations grow in amplitude over time, and the water tank level fails to stabilize near the set point. This indicates that the integral gain is too aggressive, resulting in an uncontrollable loop where the controller continuously overcorrects the error, amplifying disturbances instead of correcting them. Despite the drawbacks of higher integral gain settings, it is evident that the inclusion of the integral term successfully eliminates the offset caused by the proportional-only controller. Therefore, a lower integral gain such as $I_1=0.2 \text{ s}^{-1}$, offers the best compromise, achieving accurate set point tracking with acceptable dynamic performance.

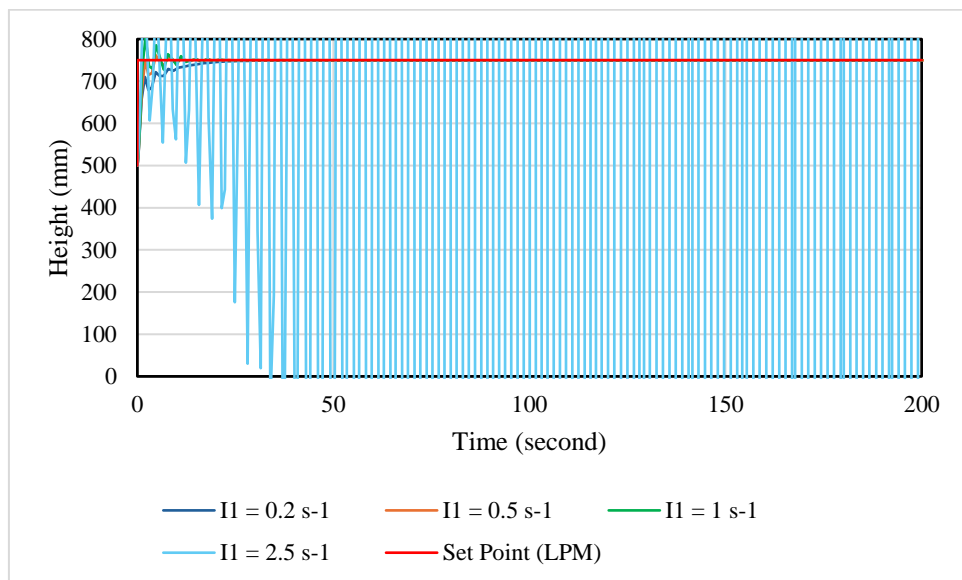


Figure 4.33: Response of simulated liquid level (controlled variable) toward the set point change (from 10 LPM to 15 LPM) regulated by proportional and integral controller with different I_I values and constant $P_I = 1$

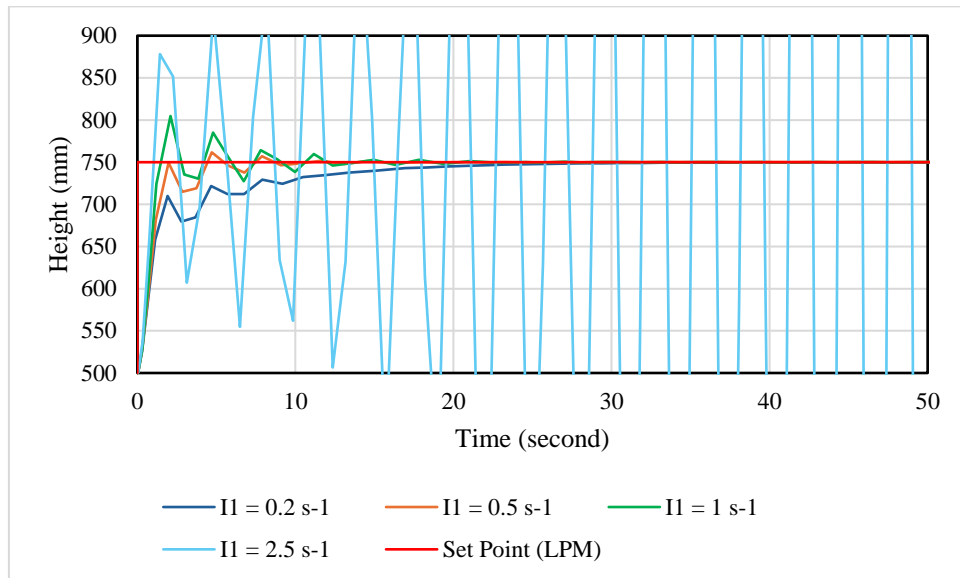


Figure 4.34: Detailed view of early-stage system response in Figure 4.33

Figure 4.35 illustrates the dynamic response of the tank level when the derivative gain D_1 in the primary level controller G_{c1} is varied. The primary level controller operates with constant values of $P_1 = 1$, $I_1 = 0.2 \text{ s}^{-1}$ and $N = 3$, and only the derivative time constant, D_1 is adjusted from 0.1 s to 10 s. As shown in Figure 4.31, when $D_1 = 0.1 \text{ s}$, the response shows almost no difference compared to Figure 4.36 when the derivative action is not utilized. As the derivative action increases to 0.5 s, the system shows a reduction in the overshoot caused by the integral action. The system reaches the set point more smoothly compared to the case in which $D_1 = 0.1 \text{ s}$. The further increment of the derivative value at $D_1 = 2.5 \text{ s}$ shows that the system becomes progressively more damped with no overshoot and the system stabilizes more quickly around the set point with minimal oscillation. At $D_1 = 10 \text{ s}$, the system response exhibits an overshoot due to the strong influence of the derivative term at the beginning of the response. The derivative component in a PID controller reacts to the rate of change of the error rather than the error itself. As the set point changes abruptly at the start of the simulation, the resulting rapid increase in error causes the derivative term to respond aggressively in an attempt to preemptively correct future deviations. While the derivative gain can improve damping and suppress overshoot, but may introduce sharp initial movements in response to sudden set point changes if tuned too aggressively. Therefore, for the cascade control system, the use of a PI controller is sufficient to

achieve effective control of the liquid level in the tank. The addition of a derivative component offers minimal improvement in performance and is not deemed necessary.

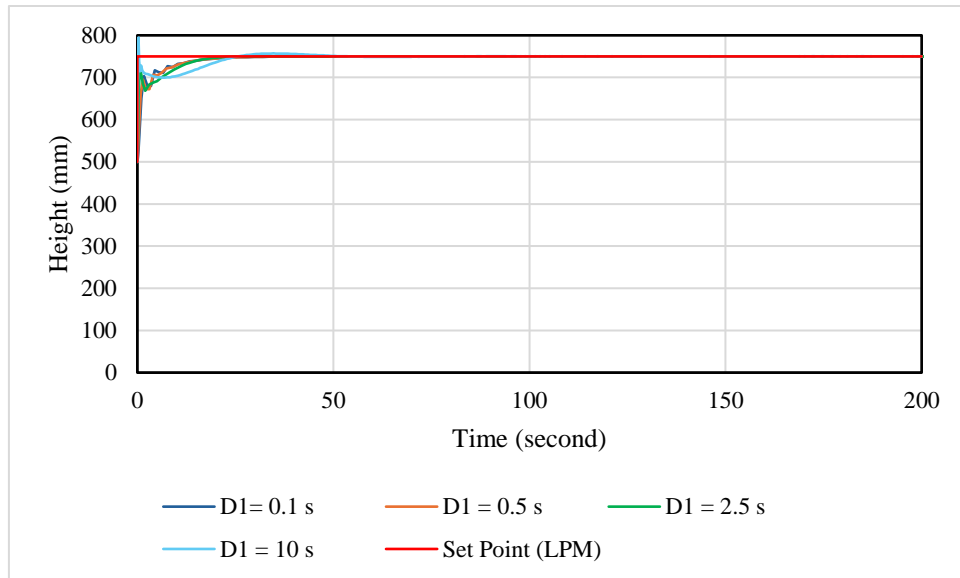


Figure 4.35: Response of simulated liquid level (controlled variable) toward the set point change (from 10 LPM to 15 LPM) regulated by proportional, integral, and derivative controller with different D values and constant $P_I = 1$ and $I_I = 0.2 \text{ s}^{-1}$

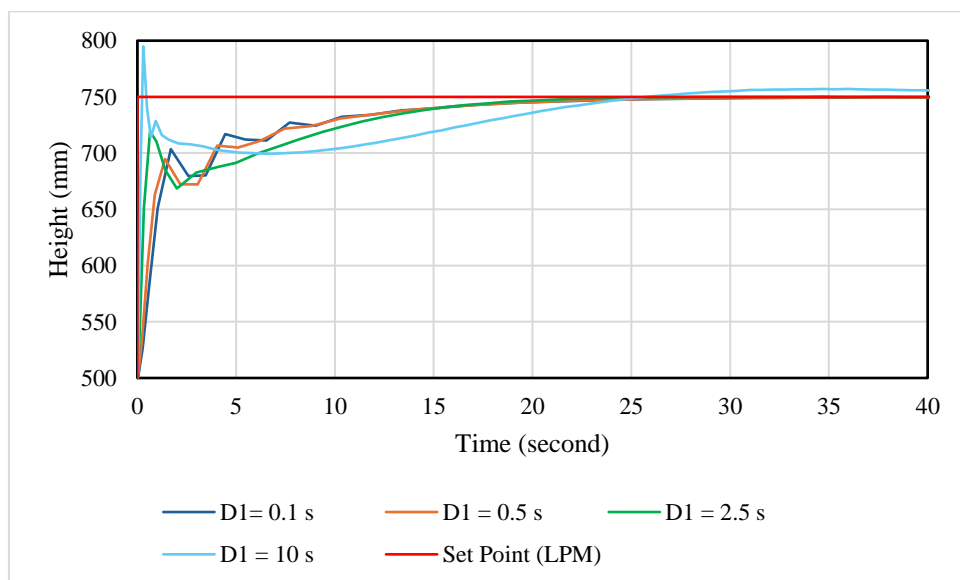


Figure 4.36: Detailed view of early-stage system response in Figure 4.35

In summary, the developed digital twin demonstrates sufficient accuracy for educational purposes, allowing users to study the effects of P, PI, and PID controllers within a flow/level cascade control system. It offers a practical platform to observe

control behavior, analyze system performance, and understand the impact of various controller settings in a simulated environment. The model's validity is further supported by consistency with the findings of Seborg et al. (2016). As the proportional gain increases, the system responds more quickly but tends to exhibit oscillations, leading to reduced stability despite a smaller steady-state offset. Despite this trade-off, proportional-only control remains attractive due to its simplicity and is suitable for applications where high precision is not essential. Integral control, on the other hand, effectively eliminates steady-state offset for all gain values. However, a very low integral gain results in a sluggish response, while a high integral gain may introduce oscillatory behavior. Derivative control can help improve system performance by reducing the maximum deviation, response time, and oscillations if the derivative time is appropriately tuned. If set too small, it may have little to no effect, while an excessively large derivative time can amplify noise and cause instability (Seborg et al., 2016).

CHAPTER 5

CONCLUSION AND RECOMMENDATION

5.1 Conclusion

This project aimed to address the limitations of traditional laboratory-based education by developing a digital twin for flow and level control systems, utilizing both feedback PID and cascade control strategies (for SOLTEQ® Flow/Level Cascade Control Trainer). The core problem identified was the inefficiency of conventional physical laboratories, which often suffer from restricted accessibility, high operational costs, and inherent safety risks. These constraints can significantly impede students' learning outcomes and practical understanding of control systems. To mitigate these challenges, the project introduced a digital twin model of a educational control unit (flow and level control system) that offers a flexible, scalable, and immersive virtual environment where students can safely and independently perform experiments without relying on physical lab infrastructure. By enhancing accessibility and promoting sustainable educational practices, this initiative aligns with the United Nations' Sustainable Development Goals (SDGs), particularly SDG 4: Quality Education and SDG 11: Sustainable Cities and Communities.

To start this project, real time experiments involving P, PI, and PID controllers for flow control were carried out and thoroughly evaluated. The experimental findings reveal that when only a P controller is used, a steady-state offset remains, although it gradually decreases as the proportional gain increases. However, this also makes the system response more aggressive and may introduce a slight overshoot. When a PI

controller is applied, the offset is eliminated, but this comes at the cost of introducing overshoot and oscillations around the setpoint before the system stabilizes. With a PID controller, the overshoot is reduced and the response becomes more damped, resulting in a smoother and more stable system behavior. Overall, the PID controller provides the best balance between accuracy and stability, making it the most effective option for minimizing both offset and oscillation.

Then, the process and associated instruments were mathematically modeled to replicate the dynamics of physical equipment. The mathematical model of the system was then derived using first principles, linearized, and transformed into transfer functions. These functions were implemented in MATLAB Simulink to create the digital twin, which was simulated and validated against the experimental data. Unknown process parameters were determined by comparing experimental outcomes with simulation data from the flow control loop. For instance, from the trial-and-error fitting between the experimental and simulation results, it is found that $K_{IP}K_V = 1$ and $\tau_V = 2.3$. With these values, the simulation of the model is conducted and it is found that the simulation results are closely aligned with real-time experimental results for the flow control system, confirming its reliability in representing the actual system.

Furthermore, the simulation on the level control system and cascade control system shows the general trend. Key findings include higher proportional gains reduced steady-state error but introduced oscillations, while lower gains resulted in slower responses and larger offsets. The integral action eliminates steady-state error but required careful tuning to avoid overshoot and instability. The derivative component had minimal impact on the fast-response system but could improve damping in slower systems. The combination of flow and level control loops enhanced system stability and responsiveness, with the inner loop mitigating disturbances before they affected the outer loop.

In conclusion, this project successfully developed a functional digital twin for flow and level control systems, including a flow/level cascade control system. The digital twin was able to replicate experimental results with reasonable accuracy, demonstrating its potential as an effective educational tool. However, some

discrepancies observed during the initial response phases for each PID controller setting indicate the need for further refinement of the model. These variations may be attributed to simplified assumptions in areas such as control valve dynamics, transducer gains, unmodeled disturbances, and external factors like pressure fluctuations and friction losses.

5.2 Recommendation

In order to enhance the digital twin's accuracy and utility, future work could:

1. Incorporate additional disturbances and external factors, such as pressure fluctuations and sensor noise, into the model.
2. Explore advanced control strategies like Model Predictive Control (MPC) or fuzzy logic for improved performance.
3. Expand the scope to include temperature and pressure control systems for a more comprehensive learning experience.

This project successfully demonstrated its potential to revolutionize engineering education by providing an accessible, cost-effective, and interactive learning platform. The findings underscore the importance of digital twins in modern education and their role in preparing students for the technological demands of Industry 4.0.

REFERENCES

- Ardabili, S.F., Mahmoudi, A., Gundoshmian, T.M. and Roshanianfard, A., 2016. Modeling and comparison of fuzzy and on/off controller in a mushroom growing hall. *Measurement*, 90, pp.127-134.
- Åström, K.J. and Murray, R., 2021. *Feedback systems: an introduction for scientists and engineers*. Princeton university press.
- Bilansky, J., Lacko, M., Pastor, M., Marcinek, A. and Durovsky, F., 2023. Improved digital twin of li-ion battery based on generic matlab model. *Energies*, 16(3), p.1194.
- Borase, R.P., Maghade, D.K., Sondkar, S.Y. and Pawar, S.N., 2021. A review of PID control, tuning methods and applications. *International Journal of Dynamics and Control*, 9, pp.818-827.
- Davies, O., Makkattil, A., Jiang, C. and Farsi, M., 2022. A digital twin design for maintenance optimization. *Procedia CIRP*, 109, pp.395-400.
- Faulconer, E.K. and Gruss, A.B., 2018. A review to weigh the pros and cons of online, remote, and distance science laboratory experiences. *International Review of Research in Open and Distributed Learning*, 19(2).
- Glatt, M., Sinnwell, C., Yi, L., Donohoe, S., Ravani, B. and Aurich, J.C., 2021. Modeling and implementation of a digital twin of material flows based on physics simulation. *Journal of Manufacturing Systems*, 58, pp.231-245.
- Harbud, N., 2022. Process automation systems. In *Integration and Optimization of Unit Operations* (pp. 191-218). Elsevier.
- He, R., Chen, G., Dong, C., Sun, S. and Shen, X., 2019. Data-driven digital twin technology for optimized control in process systems. *ISA transactions*, 95, pp.221-234.
- Huilcapi, V., Blasco, X., Herrero, J.M. and Reynoso-Meza, G., 2019. A loop pairing method for multivariable control systems under a multi-objective optimization approach. *IEEE Access*, 7, pp.81994-82014.
- Irimia, C., Grovu, M., Sirbu, G.M., Birtas, A., Husar, C. and Ponchant, M., 2019, October. The modeling and simulation of an Electric Vehicle based on Simcenter Amesim platform. In *2019 Electric Vehicles International Conference (EV)* (pp. 1-6). IEEE.

- Ito, A., Oetinger, P., Tasaki, R., Sawodny, O. and Terashima, K., 2018, July. Visual nonlinear feedback control of liquid level in mold sprue cup by cascade system with flow rate control for tilting-ladle-type automatic pouring system. In *Materials Science Forum* (Vol. 925, pp. 483-490). Trans Tech Publications Ltd.
- Joe, J. and Karava, P., 2019. A model predictive control strategy to optimize the performance of radiant floor heating and cooling systems in office buildings. *Applied Energy*, 245, pp.65-77.
- Johra, H., Petrova, E.A., Rohde, L. and Pomianowski, M.Z., 2021, November. Digital twins of building physics experimental laboratory setups for effective e-learning. In *Journal of Physics: Conference Series* (Vol. 2069, No. 1, p. 012190). IOP Publishing.
- Kathane, B.Y., Dahikar, P.B. and Sharma, S.J., 2013. Upcoming Trends of Virtual Experiments for Laboratories. *International Journal of Computer Science and Business Informatics*, 2(1), pp.1-14.
- Kazała, R., Luściński, S., Strączyński, P. and Taneva, A., 2021. An enabling open-source technology for development and prototyping of production systems by applying digital twinning. *Processes*, 10(1), p.21.
- Kiyakli, A.O. and Solmaz, H., 2019. Modeling of an electric vehicle with MATLAB/Simulink. *International journal of automotive science and technology*, 2(4), pp.9-15.
- Mikkili, S., Panda, A.K. and Prattipati, J., 2015. Review of real-time simulator and the steps involved for implementation of a model from MATLAB/SIMULINK to real-time. *Journal of The Institution of Engineers (India): Series B*, 96, pp.179-196.
- Padula, F., Ionescu, C., Latronico, N., Paltenghi, M., Visioli, A. and Vivacqua, G., 2017. Optimized PID control of depth of hypnosis in anesthesia. *Computer methods and programs in biomedicine*, 144, pp.21-35.
- Pires, F., Cachada, A., Barbosa, J., Moreira, A.P. and Leitão, P., 2019, July. Digital twin in industry 4.0: Technologies, applications and challenges. In *2019 IEEE 17th international conference on industrial informatics (INDIN)* (Vol. 1, pp. 721-726). IEEE.
- Rodemann, T. and Unger, R., 2018. Smart company digital twin-supporting controller development and testing using FMI. In *Proceedings of the Japanese Society of Automotive Engineers Spring Meeting*. Yokohama, Japan: JSAE.
- Seborg, D.E., Edgar, T.F., Mellichamp, D.A. and Doyle III, F.J., 2016. *Process dynamics and control*. John Wiley & Sons.

- Schluse, M., Priggemeyer, M., Atorf, L. and Rossmann, J., 2018. Experimentable digital twins—Streamlining simulation-based systems engineering for industry 4.0. *IEEE Transactions on industrial informatics*, 14(4), pp.1722-1731.
- Semeraro, C., Lezoche, M., Panetto, H. and Dassisti, M., 2021. Digital twin paradigm: A systematic literature review. *Computers in Industry*, 130, p.103469.
- Shukla, A., Khare, M. and Shukla, K.N., 2015. Modeling and simulation of solar PV module on MATLAB/Simulink. *International Journal of Innovative Research in Science, Engineering and Technology*, 4(1).
- Urica, T., Sojka, P., Koniar, D. and Hargas, A.S.L., 2019, May. The control process of an on-off controller. In *2019 20th International Scientific Conference on Electric Power Engineering (EPE)* (pp. 1-6). IEEE.
- VanDerHorn, E. and Mahadevan, S., 2021. Digital Twin: Generalization, characterization and implementation. *Decision support systems*, 145, p.113524.
- Wang, T., Gao, H. and Qiu, J., 2015. A combined adaptive neural network and nonlinear model predictive control for multirate networked industrial process control. *IEEE Transactions on Neural Networks and Learning Systems*, 27(2), pp.416-425.
- Wu, J., Zhang, B., Wang, L. and Yu, G., 2021. An iterative learning method for realizing accurate dynamic feedforward control of an industrial hybrid robot. *Science China Technological Sciences*, 64(6), pp.1177-1188.
- Yang, C., Xie, Y., Liu, S. and Sun, D., 2018. Force modeling, identification, and feedback control of robot-assisted needle insertion: a survey of the literature. *Sensors*, 18(2), p.561.
- Yang, Y., Meng, W. and Zhu, S., 2020, November. A digital twin simulation platform for multi-rotor UAV. In *2020 7th International Conference on Information, Cybernetics, and Computational Social Systems (ICCSS)* (pp. 591-596). IEEE.